(12) INTERNATIONAL APPLICATION PUBLISHED UNDER THE PATENT COOPERATION TREATY (PCT)

(19) World Intellectual Property Organization
International Bureau

(43) International Publication Date
11 August 2005 (11.08.2005)

PCT

(10) International Publication Number
WO 2005/072630 A1

(51) International Patent Classification[7]: A61B 17/20, A61M 37/00

(21) International Application Number: PCT/GB2005/000336

(22) International Filing Date: 31 January 2005 (31.01.2005)

(25) Filing Language: English

(26) Publication Language: English

(30) Priority Data:
0402131.7 30 January 2004 (30.01.2004) GB

(71) Applicant *(for all designated States except US)*: **ISIS INNOVATION LIMITED** [GB/GB]; Ewert House, Ewert Place, Summerton, Oxford Oxfordshire OX2 7SG (GB).

(72) Inventor; and

(75) Inventor/Applicant *(for US only)*: **KENDALL, Mark** [GB/GB]; Department of Engineering, Parks Road, Oxford Oxfordshire OX1 3PJ (GB).

(74) Agents: **BALDOCK, Sharon, Claire** et al.; BOULT WADE TENNANT, Verulam Gardens, 70 Gray's Inn Road, London WC1X 8BT (GB).

(81) Designated States *(unless otherwise indicated, for every kind of national protection available)*: AE, AG, AL, AM, AT, AU, AZ, BA, BB, BG, BR, BW, BY, BZ, CA, CH, CN, CO, CR, CU, CZ, DE, DK, DM, DZ, EC, EE, EG, ES, FI, GB, GD, GE, GH, GM, HR, HU, ID, IL, IN, IS, JP, KE, KG, KP, KR, KZ, LC, LK, LR, LS, LT, LU, LV, MA, MD, MG, MK, MN, MW, MX, MZ, NA, NI, NO, NZ, OM, PG, PH, PL, PT, RO, RU, SC, SD, SE, SG, SK, SL, SY, TJ, TM, TN, TR, TT, TZ, UA, UG, US, UZ, VC, VN, YU, ZA, ZM, ZW.

(84) Designated States *(unless otherwise indicated, for every kind of regional protection available)*: ARIPO (BW, GH, GM, KE, LS, MW, MZ, NA, SD, SL, SZ, TZ, UG, ZM, ZW), Eurasian (AM, AZ, BY, KG, KZ, MD, RU, TJ, TM), European (AT, BE, BG, CH, CY, CZ, DE, DK, EE, ES, FI, FR, GB, GR, HU, IE, IS, IT, LT, LU, MC, NL, PL, PT, RO, SE, SI, SK, TR), OAPI (BF, BJ, CF, CG, CI, CM, GA, GN, GQ, GW, ML, MR, NE, SN, TD, TG).

Declaration under Rule 4.17:
— *of inventorship (Rule 4.17(iv)) for US only*

Published:
— *with international search report*

For two-letter codes and other abbreviations, refer to the "Guidance Notes on Codes and Abbreviations" appearing at the beginning of each regular issue of the PCT Gazette.

(54) Title: DEVICE FOR DELIVERY OF BIOACTIVE MATERIALS AND OTHER STIMULI

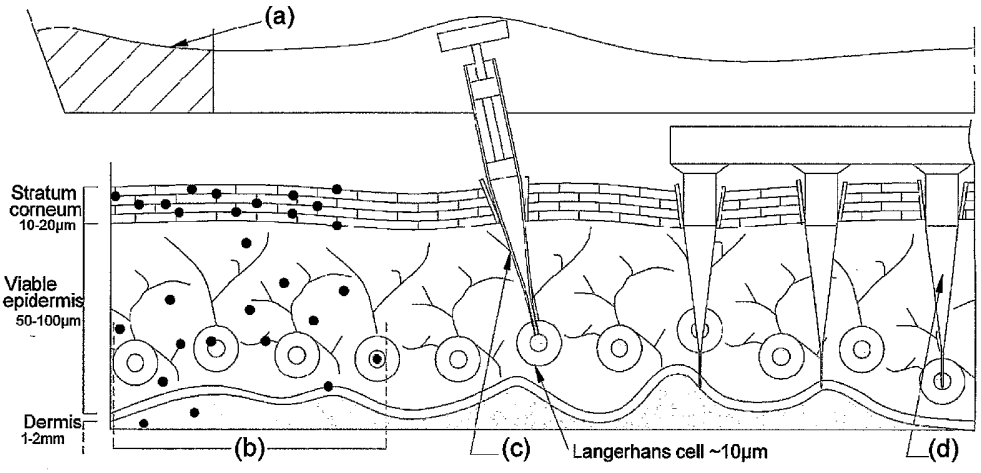

(57) Abstract: The present invention relates to devices for delivering bioactive substances and other stimuli to living cells, to methods of manufacture of the device and to various uses of the device, including a number of medical applications. The device comprises a plurality of projections which can penetrate a body surface so as to deliver the bioactive material or stimulus to the required site, wherein the projections are solid and the delivery end section of the projection is so dimensioned as to be capable of insertion into targeted cells to deliver the bioactive material or stimulus without appreciable damage to the targeted cells or specific sites therein.

WO 2005/072630 A1

Device for delivery of bioactive materials and other stimuli

Field of the Invention

This invention relates to devices for delivering bioactive substances and other stimuli to living cells, to methods of manufacture of the device and to various uses of the device.

Introduction

In recent years, attempts have been made to devise new methods of delivering drugs and other bioactive materials, for vaccination and other purposes, which provide alternatives that are more convenient and/or enhanced in performance to the customary routes of administration such as intramuscular and intradermal injection. Limitations of intradermal injection include: cross-contamination through needle-stick injuries in health workers; injection phobia from a needle and syringe; and most importantly, as a result of its comparatively large scale and method of administration, the needle and syringe cannot target key cells in the outer skin layers (Figure 1(a)). This is a serious limitation to many existing and emerging strategies for the prevention, treatment and monitoring of a range of untreatable diseases.

The skin structure is shown in Figure 1, with a summary of key existing delivery methods. Non-invasive methods of delivery through the skin have been used, including patches, liquid solutions and creams. Their success is dependant upon the ability to breach the semi-permeable stratum corneum (SC) into the viable epidermis. Typically, larger biomolecules are unable to breach this barrier.

Alternatively, there are many more "invasive" means to breach the SC for pharmaceutical delivery to the viable epidermis. Simple methods include: tape stripping with an abrasive tape or sandpaper and the application of depilatory agents. Amongst the more advanced technologies are electroporation, ablation by laser or heat, radiofrequency high voltage currents, iontopheresis, liposomes, sonophoresis. Many of these approaches remain untested for complex entities such as vaccines and

immunotherapies. Moreover, they do not specifically deliver entities *within* key skin cells.

Needle-free *injection* approaches include the high-speed liquid jet injector, which had a rise and fall in popularity in the mid twentieth century—and has recently seen a resurgence (Furth, P.A., Shamay, A. & Henninghausen, L. (1995) Gene transfer into mammalian cells by jet injection. *Hybridoma*, 14:149–152.). However, this method delivers jets of liquid to the epidermis and dermis (labelled (c) in Fig A), usually with a diameter >100 μm—and not within key cells. Furthermore, as a result of the concentrated jet momentum, many skin cells die. Delivery into the dermis also leads to patients reporting pain from injection.

The ballistic, needle-free delivery of microparticles (or gene gun) offers a route for delivering biological agents directly into cells of the skin. In this needle-free technique, pharmaceutical or immunomodulatory agents, formulated as or coated to particles, are accelerated in a high-speed gas jet at sufficient momentum to penetrate the skin (or mucosal) layer and to achieve a pharmacological effect. A schematic of microparticles in the skin following biolistic delivery is shown in Figure 1(b). The ability of this "scatter gun" approach to deliver genes and drugs to epidermal cells is highly limited and sensitive to biological variability in skin properties on the dynamic high strain rate ballistics process. These effects are discussed in Kendall, M.A.F., Rishworth, S., Carter, F.V. & Mitchell, T.J. (2004) The effects of relative humidity and ambient temperature on the ballistic delivery of micro-particles into excised porcine skin. *J. Investigative Dermatology*, 122(3):739–746.).; and Kendall, M.A.F., Mitchell, T.J. & Wrighton-Smith, P. (2004) Intradermal ballistic delivery of micro-particles into excised human skin for drug and vaccine applications. *J. Biomechanics*, 37(11):1733–1741.

First, the ballistic delivery of particles into the skin to target epidermal cells is extremely sensitive to the small variations in the stratum corneum—including the stratum corneum thickness, which varies massively with body site, age, sex, race and exposure to climatic conditions. (The quasi-static loading of skin with micro-nanostructures would be less sensitive to these differences).

Second, it has been shown that even when all these parameters are strictly controlled—and the only parameter varied is the climatic relative humidity (15%-95%), or, independently, temperature (20°C-40°C)—the result is a large variation in penetration depth. These results are shown in Fig. 2, with particle penetration as a function of ambient relative humidity (Fig. 2(a)) and ambient temperature (Fig. 2(b)) plotted along with theoretical calculations of particle penetration and measured stratum corneum thickness. This variation alone is significant and sufficient to make the difference between particles breaching the stratum corneum, or not.

The compound effect of these two (and other) sources of variability is the gene gun/biolistics process does not consistently target epidermal cells—leading to inconsistent biological responses (e.g. in DNA vaccination).

Interestingly, it has also been shown that the high strain-rate loading of the skin under ballistic particle impact (approximately 10^6 per second) increases the stratum corneum breaking stress by up to a factor of 10 compared to quasi-static values—due to a ductile-to-brittle change in the skin mechanical properties. This means that the tissue is more difficult to penetrate as the particle impact velocity is increased. Therefore it is desirable to devise a way to deliver micro/nanostructures to the skin at lower strain-rates than the ballistic approach to exploit the weaker stratum corneum.

When the microparticles are delivered to the skin, it is unclear whether there are any adverse longer term effects. For example, in the case of insoluble particles, many of them slough off with the usual skin turnover. However, gold particles have been detected in the lymph nodes following ballistic particle delivery—presumably by migration with Langerhans cells. Uncertainty of adverse effects of these delivered materials would be removed by delivery routes that do not leave such materials in tissue site.

Moreover, when the microparticles successfully target cells, there is a significant probability they kill the cells they target. Consider a typical ballistic delivery condition: over 1 million 2-3 μm diameter gold particles coated in DNA to the skin at 400—600 m/s, over a target diameter of 4 mm (Kendall, M.A.F., Mulholland, W.J., Tirlapur, U.K., Arbuthnott, E.S. & Armitage, M. (2003) Targeted delivery of micro-particles to epithelial cells for immunotherapy and vaccines: an experimental and probabilistic study. *6th International Conference on Cellular Engineering*. August 20–22 2003, Sydney, Australia.). Reported experiments with these conditions using

cell death stains (ethidium bromide/acridin orange) show that microparticles impacting the skin do kill cells (McSloy, N.J., Raju, P.A. & Kendall, M.A.F. (2004) The effects of shock waves and particle penetration in skin on cell viability following gene gun delivery. *British Society for Gene Therapy, 1st Annual Conference.* Oxford, UK, March 28–30 2004; Raju, P.A. & Kendall, M.A.F. (2004) Epidermal cell viability following the ballistic delivery of DNA vaccine microparticles. *DNA Vaccines 2004—the Gene Vaccine Conference.* 17–19 November 2004, Monte Carlo, Monaco.).

Fig. 3(a) shows the percentage of cells that had membrane rupture (i.e. death) as a function of the localised particle channel density. In Fig. 3(b) we see schematically the way the data in Fig. 3(a) was achieved, relating "tracks" left by particle penetration to the death of cells in a layer of the viable epidermis. Clearly, Figure 3(a) shows that at a channel density above 0.01 channels/micron, all the cells in that layer are dead. Indeed, Figure 3(c) shows that cells are killed when the particle is passing up to 10 μm *outside* of the cell boundary. The mechanism of cell death is due to the propagation of stress and shock waves in the skin generated by the rapid deceleration of the microparticles (McSloy et al. (2004)). The rapid rise time of these stress waves in the skin, and their magnitude both contribute to cell death and the results are consistent with the findings reported by Doukas, A.G. & Flotte, T.J. (1996) Physical characterisation and biological effects of laser-induced stress waves. *Ultrasound in Medicine and Biology*, 22(2):151–164. The effects of shock waves and particle penetration in the skin on cell viability following gene gun delivery. *Masters Thesis*, Department of Engineering Science, University of Oxford.). This mechanism of ballistic particle penetration killing cells negatively affects the ability of the direct and efficient delivery of genes and drugs to the cells.

This cell death effect of ballistic particle delivery could be reduced by significantly decreasing the particle size to the nanometre regime—thereby reducing the stresses on the cells. However, another limitation of the gene gun is that it is unsuitable in delivering sub-micron sized particles to cells. This is illustrated by the following. As reported (Kendall, M.A.F., Mitchell, T.J. & Wrighton-Smith, P. (2004) Intradermal ballistic delivery of micro-particles into excised human skin for drug and vaccine applications. *J. Biomechanics*, 37(11):1733–1741), and shown in Figure 4, ballistic

particle penetration is proportional to the particle impact parameter, ρvr, which is the product of the particle density (ρ), velocity (v) and radius (r). This parameter is also proportional to the particle momentum per-unit-area, which has been shown to drive the mechanism of particle penetration depth (Mitchell et al. (2003)). From Figure 4, we see a 1 μm radius gold particle (density 18000 kg/m^3) would need to impact the skin at ~600 m/s in order to penetrate to reach cells ~20 μm into the skin. Experimental results show that reducing the particle radius, say, by an order of magnitude, to 100 nm, and placing it in a standard biolistic device leads to negligible particle impact in the skin. Indeed from Figure 4 we see delivery to a 20 μm depth would need an impact velocity of ~6000 m/s, which is impractical for two reasons: 1) these hypervelocity conditions can not be safely achieved with a system configured for human use (they are usually achieved with massive free-piston shock tunnels); 2) even if 6000 m/s was obtained in the free-jet, a gas impingement region above the skin would seriously decrease the particle velocity—it is possible that the particle would not even hit the skin at all. Interestingly if a method was conceived to safely and practically deliver nanoparticles to the skin at higher velocity (e.g. the stated case of a ~100 nm radius gold particle at a velocity of ~6000 m/s), the cell death benefit of smaller scale would be offset by higher peak stresses—killing more cells—and higher strain rates that are likely to further "toughen" the skin, making delivery even more difficult.

In conclusion, these collective facts rule out the gene gun as a viable option for delivering nanoparticles and therefore precludes it from many of the developments in biomolecules, drugs and sensors at this scale.

The huge research effort in micro- and nanotechnologies provides tremendous potential for simple and practical cell targeting strategies to overcome many limitations of current biolistic (and other) cell targeting approaches. For example, Figure 1(c) shows that the most conceptually simple and appealing approach to gene delivery is the direct injection of naked DNA to live cell nuclei at a sub-micrometre scale that does not adversely damage the cell (Luo, D. & Saltzman, W.M. (2000) Synthetic DNA delivery systems. *Nature Biotechnology*, 18:33–36). Cell death is minimised by both the sub-micrometre scale of the injector and the low, quasi-static strain-rate of the probe (compared to ballistic delivery) resulting in low stress

distributions. Although this is a very efficient gene and bioagent delivery route, the drawback is that such precise targeting by direct microinjection can only be achieved one cell at a time and with great difficulty to the operator *in vivo*. Hence, the method is slow, laborious and impractical.

Researchers have overcome some of these disadvantages by fabricating arrays of micrometre-scale projections (thousands on a patch) to breach the stratum corneum for the intradermal delivery of antigens and adjuvants to humans and other mammals.

In the scientific literature, the first description of this technique appears to be the paper 'Microfabricated Microneedles : A Novel Approach to Transdermal Drug Delivery. S.Henry *et al*, J.Pharmaceutical Sci. vol 87(8) p922-925 (1998), with the accompanying patent of US 6,503,231. The objective of US 6,503,231 is to provide a microneedle array device for relatively painless, controlled, safe, convenient transdermal delivery of a variety of drugs and for biosampling. This is achieved by the microneedles breaching the tissue barrier (e.g. for skin: the stratum corneum) and then the therapeutic or diagnostic material is injected through the hollow microneedles into the tissue. Specifically, in claim 1 of US 6,503,231, it is stated that the microneedles are to be hollow, with a length of 100 μm—1 mm, and claim 3 states the width of 1 μm-100 μm, with subsequent claims stating ways the hollow needles can be connected to reservoirs for the injection of liquids, fabrication methods, materials and examples of drugs to be delivered. Other related microneedle devices in the patent literature are US patents 5,527,288 and 5,611,806. More recently published patent applications on this topic are WO 02/085446, WO 02/085447, WO 03/048031, WO 03/053258 and WO 02/100476 A2.

These microneedles array patch technologies have achieved only limited success to date. Generally, there are a range of approaches configured to breach the stratum corneum to allow an enhanced take-up of drug in the viable epidermis. Although this has not been discussed in the patents referred to above, based upon reported research on ballistic particle delivery and cell death, the low strain rate of application, combined with the cases of smaller projections are likely to induce a lower incidence of cell death near the tips, than ballistic microparticle delivery. Also, unlike ballistic

microparticle delivery, these projections are removed from the tissue—alleviating the possibility of adverse effects of "carrier" materials delivered to the body, long term.

However, unlike biolistic targeting (Figure 1(b)), and the direct injection of cells (Figure 1(c)), these microneedle arrays do not have the advantage of readily and directly targeting *inside* the skin cells. This cellular/organelle targeting capability is key in a range of existing and potential methods of vaccination, gene therapy, cancer treatment and immunotherapy (Needle-free epidermal powder immunization. Chen *et al,* Expert Rev. Vaccines 1(3) p265–276 (2002)) and diagnostic technologies.

Therefore, there still remains a need to provide projection-based technology which achieves a more accurately directed delivery of the active agent or stimulus to the desired site of action *within* cells, without appreciable damage to them.

The present invention comprises a device for the delivery of a bioactive material (agent) or other stimulus to an internal site in the body, comprising a plurality (number) of projections which can penetrate a body surface so as to deliver the bioactive material or stimulus to the required site, wherein the delivery end portion of the projection is so dimensioned as to be capable of insertion into targeted cells to deliver the bioactive material or stimulus without appreciable damage to the targeted cells or specific sites therein.

An important distinction from the devices described in the above mentioned patents and publications on microprojection array technology is the much reduced dimensions of the delivery end portion of the microprojections, both as to length and width, which enables delivery of the agent or stimulus to targeted cells and internal components within cells. Thus, whereas the typical length of the microneedles of the prior devices is measured in microns e.g. less than 500 microns, the delivery end point of those of the present invention is usually no more than a few microns in length and frequently chosen with a diameter at nanometre scale. The needles used at this very small scale are therefore to be referred to hereinafter as nanoneedles.

The nanoneedles are solid (non-hollow) in cross-section. This leads to a number of technical advantages which include: reliable delivery of bioactive material or stimulus; ease and cost of manufacturing, and increased strength.

Herein, the terms "projection", "micro-nanoprojection", "nanoneedle", "nanoprojection", "needle", "rod" etc are used interchangeably to describe the solid projections which form an essential part of the invention. An example of such a projection is provided in Figure 10 and is described in more detail below.

In cases where a material or agent is to be transported, these may be coated on the outside of the nanoneedles. This provides a distinguishing and advantageous feature of a higher probability of delivering the coating to the depth of interest compared to microparticle delivery from a gene gun—and thus is more efficient.

A further distinguishing and advantageous feature is that the nanoneedles may be used for delivery not only through the skin but through other body surfaces, including mucosal surfaces, to cellular sites below the outer layer or layers of such surfaces. The term "internal site", as used herein, is to be understood as indicating a site below the outer layer(s) of skin and other tissues for which the devices of the present invention are to be used.

Furthermore, these nanoneedles may be used to deliver stimuli to cells or cell components other than those resulting from the administration of bioactive agents such as drugs and antigenic materials for example. Mere penetration of cellular sites with nanoneedles may be sufficient to induce a beneficial response, as indicated hereinafter.

The device of the invention is suitable for intracellular delivery. The device is most preferably suitable for delivery to specific organelles within cells. Examples of organelles to which the device can be applied include a cell nucleus, endoplasmic reticulum, ribosome, or lysosome for example.

In one embodiment the device is provided having a needle support section, that is to say the projections comprise a suitable support section, of sufficient length to reach

the desired site and a (needle) delivery end section having a length no greater than 20 microns and a maximum width no greater than 5 microns, preferably no greater than 2 microns.

Preferably, the maximum width of the delivery end section is no greater than 1000 nm, even more preferably the maximum width of the delivery end section is no greater than 500 nm.

In one embodiment, the device of the invention is for delivery intradermally. Preferably this device has a needle support section, that is to say the projections comprise a suitable support section, of length at least 10 microns and a (needle) delivery end section having a length no greater than 20 microns and a maximum width no greater than 5 microns, preferably no greater than 2 microns.

Preferably, the maximum width of the delivery end section is no greater than 1000 nm, even more preferably the maximum width of the delivery end section is no greater than 500 nm.

In a further embodiment, the device is for mucosal delivery. Preferably this device has a needle support section, that is to say the projections comprise a suitable support section, of sufficient length to reach the desired site, preferably of length at least 100 microns and a (needle) delivery end section having a length no greater than 20 microns and a maximum width no greater than 5 microns, preferably no greater than 2 microns.

Preferably, the maximum width of the delivery end section is no greater than 1000 nm, even more preferably the maximum width of the delivery end section is no greater than 500 nm.

In one embodiment, the device of the invention is for delivery to lung or other internal organ or tissue. In a further embodiment, the device is for in-vitro delivery to tissue, cell cultures, cell lines, organs, artificial tissues and tissue engineered products. Preferably this device has a needle support section, that is to say the projections comprise a suitable support section, of length at least 5 microns and a needle delivery

end section having a length no greater than 20 microns and a maximum width no greater than 5 microns, preferably no greater than 2 microns.

Even more preferably, the width of the delivery end section is no greater than 1000 nm, and most preferably no greater than 500 nm.

In a most preferred embodiment, the device of the invention comprises projections in which the (needle) delivery end section and support length, that is to say the "needle support section", is coated with a bioactive material across the whole or part of its length. Preferably, the (needle) delivery end section and support length is coated on selective areas thereof. This may depend upon the bioactive material being used or the target selected for example.

In a further embodiment, a bioactive material is releasably incorporated into the material of which the needle, or projection, is composed. All, or part of the projection may be constructed of a biocompatible, biodegradable polymer (such as Poly Lactic Acid (PLA), Poly Glycolic Acid (PGA) or PGLA or Poly Glucleic Acid), which is formulated with the bioactive material of choice. The projections may then be inserted into the appropriate target site and, as they dissolve, the bioactive material will enter the organelle(s)/cells.
Preferably, at least the delivery end section of the needle is composed of a biodegradable material.

In an alternative embodiment of the invention, a device is also provided in which the needle has no bioactive material on or within it. The targeted cell or organelle is perturbed/stimulated by the physical disruption caused by the (delivery end of the) nanoneedle (projection). This physical stimulus may, for example, be coupled with electric stimulus as a form of specific nanoelectroporation of particular organelles or the cell.

The bioactive material or stimulus delivered by the device of the invention may be any suitable material or stimulus which gives the desired effect at the target site. Examples of bioactive materials, which are not intended to be limiting with respect to the invention include polynucleotides and nucleic acid or protein molecules, antigens,

allergens, adjuvants, molecules, elements or compounds. In addition, the device may be coated with materials such as biosensors, nanosensors or MEMS.

In one preferred aspect of the invention, the device is provided in the form of a patch containing a plurality of needles (projections) for application to a body surface. A multiplicity of projections can allow multiple cells and organelles to be targeted and provided with a bioactive material or stimulus at the same time. The patch may be of any suitable shape, such as square or round for example. The overall number of projections per patch depends upon the particular application in which the device is to be used. Preferably, the patch has at least 10 needles per mm^2, and more preferably at least 100 needles per mm^2. Considerations and specific examples of such a patch are provided in more detail below.

In addition, the invention also provides for the manufacture of the device of the invention. The specific manufacturing steps are described in greater detail below. In one preferred aspect, the device of the invention is constructed from biocompatible materials such as Titanium, Gold, Silver or Silicon, for example. This is preferably the entire device, or alternatively it may only be the projections or the delivery end section of the projections which are made from the biocompatible materials.

A preferred manufacturing method for the device utilises the Deep Reactive Ion Etching (DRIE) of the patterns direct from silicon wafers, see the construction section below.

Another preferred manufacturing method for the device utilises manufacturing from a male template constructed with X-ray lithography, electrodeposition and moulding (LIGA). The templates are then multiply inserted into a soft polymer to produce a plurality of masks. The masks are then vacuum deposited/sputtered with the material of choice for the nanoprojections, such as titanium, gold, silver, or tungsten. Magnetron sputtering may also be applied, see the construction section below.
An alternative means for producing masks is with 2 photon Stereolithography, a technique which is known in the art and is described with reference to the device of the invention in more detail below.

In one embodiment, the device is constructed of silicon.

The device of the invention may be for a single use or may be used and then recoated with the same or a different bioactive material or other stimulus, for example.

In one embodiment of the invention, the device comprises projections which are of differing lengths and/or diameters (or thicknesses depending on the shape of the projections) to allow targeting of different targets within the same use of the device. An example of the practical application of such a device is explained in further detail below (see section 6.2.4).

Also provided throughout the specification are numerous uses of the device of the invention, which has many useful medical applications in the treatment of a number of diseases.

In order that the present invention may be more clearly understood as to matters of principle as well as to methods of construction and use thereof, explanatory sections are provided below. Illustrative accompanying drawings and figures are provided, as follows: -

Figure 1 Schematic cross-section of skin structure: (a) half-section scale of a typical smaller needle and syringe (diameter ~0.5 mm); (b) penetration of microparticles following biolistic delivery; (c) idealised direct injection of a cell nucleus; (d) a micro-nanoprojection array.

Fig. 2. The effects of relative humidity (a) and ambient temperature (b) on ballistic particle penetration into the skin.

Fig. 3. (a) A graph showing the relationship between percentage cell death (membrane rupture) and particle density. (b) A diagram showing how the data for (a) was retrieved. (c) A graph showing membrane rupture versus distance of cell pathway.

Fig. 4. The particle penetration parameter (ρvr) vs. penetration depth obtained by the ballistic delivery of gold microparticles into skin (Kendall et al. (2004), Journal of Biomechanics). The particles are grouped into size groups and compared with calculations using a unified penetration model. The stratum corneum thickness is also shown.

Fig 5: The organelles within the cell. (http://niko.unl.edu/bs101/notes/chapter4.html).

Fig 6: A schematic of the skin.

Fig 7: A histology micrograph of human skin with a Langerhans Cell (L) and Keratinocyte (K) stained. From Roitt *et al.* The height of the monograph is approximately 50 μm.

Fig 8: The distribution of Langerhans Cells in a mouse ear (Kendall M.A.F., Mulholland W.J., Tirlapur U.K., Arbuthnott E.S., and Armitage, M. (2003) "Targeted delivery of micro-particles to epithelial cells for immunotherapy and vaccines: an experimental and probabilistic study", The 6th International Conference on Cellular Engineering, Sydney, August 20-22).

Fig 9: A sample of canine buccal mucosal tissue and the structure of the mucosa, Mitchell, T (2003) Dphil Thesis, Department of Engineering Science, University of Oxford.

Fig 10: Shape and dimensions of the nanoneedle.

Fig 11: The maximum needle length vs. nanoneedle diameter calculated using expression (3) and the Young's Modulus (E) values for Gold, Titanium, ZnO, PGCA, Silver and Tungsten (respectively: 77.2, 116, 111.2 and 7 GPa).

Fig. 12: A photograph of the electropolishing set-up for fabricating individual tungsten micro-nanoprojections.

Fig. 13: Transmission Electron Micrographs (TEM) of a micro-nanoprojection electropolished from tungsten at (a) X 500 magnification and (b) 88000 magnification.

Fig. 14: Fluorescent microscope images of tungsten rods, (a) uncoated and (b) coated in eGFP plasmid DNA immersed in an ethidium bromide solution.

Fig. 15: An optically sectioned Multi-Photon Microscopy (MPM) images of the agar after insertion of a DNA coated tungsten probe (a) on the surface (b) at a depth of 13 μm (c) at a depth of (32 μm). Also shown in (d) is an optical section at 32 μm of agar gel following insertion of a probe without a DNA coating.

Fig. 16: Photomicrograph of a micro-nanoprojection electropolished from tungsten used in skin tissue indentation experiment with scale bar.

Fig. 17: Two sample load-displacement curves in freshly excised mouse ear tissue obtained with the micro-nanoprojection shown in Fig. 16.

Fig 18: Plan view diagram of possible alternative geometry of the nanoneedle.

Fig 19: The nanoneedle array or patch device.

Fig 20: A schematic of the nanoneedle array produced with 2PLSM

Fig 21: Sequence for producing a mask. The alternative is the 2PSL.

Fig 22: "Stepped" nanoneedle.

Fig. 23: Example of an intradermal application of nanoneedle patches.

Fig. 24: Applicator, fitted with the patch for mucosal delivery.

Fig. 25: A schematic of the major respiratory organs.

Fig. 26: A deployable patch structure for targeting the lower airway and lung.

1. Specific Targets For Delivery

To illustrate the function of the invention and the importance of the nanoneedle size in targeting cells, the size of cells and key organelles is described.

The target of interest is within the cells. The position and shape of key organelles within the cells are shown in Figure 5. All eucaryotic cells have the same basic set of membrane enclosed organelles. The number and volume of the key organelles varies with cell type. As to the targetting of specific organelles, there is a probability attached to each event on the basis of volume. Consider the non-specific targeting of the cell (i.e. at the correct depth, but without the precise targeting with the aid of imaging techniques). The probability of targeting the nucleus , for example, in a cell is given by the volume of the nucleus vs. the remainder of the cell.

In Table 1 below, the scale of organelles and their mass fraction and number are listed. The primary data for this summary is from from "Genes VI" by Benjamin Lewin and "The Molecular Biology of the Cell" Alberts et al., 4th Ed. This information pertains to the Liver Cell. Also listed in Table 1 are example applications and that may be induced or enhanced as a result of targeting these organelles.

Working in increasing scale, the starting point is the cell membrane, which is ~10 nm thick. In piercing these membranes with a minimal disruption to the viability of the cell, a range of drugs, vaccines and other compounds can be delivered to cells. Specifically, the Endoplasmic Reticulum (a convoluted envelope, 75 nm in thickness) may be targeted with mRNA to transfect cells in the areas of Vaccination or Gene Therapy. Lysosomes, which are 200-500 nm in size can be targeted for release of enzymes to induce autolysis (cell death). For an effective cellular response (MHC Class I) with DNA vaccination and gene therapy, it is important that the DNA material is delivered intact to the cell nucleus.

Most of these organelles are of the submicron scale.

Table 1: The scale, number and potential targets of key organelles within cells. (http://niko.unl.edu/bs101/notes/sizes.html and "Molecular Biology of the Cell" 4th Ed, Alberts et al.)

Scale	Organelle	Mass/ Volume Fraction	Number per cell	Utility as target	Application
~0.1 nm	Hydrogen Atom				
~0.8 nm	Amino Acid				
~2 nm (diameter)	DNA Alpha helix	~2%			
~2 nm	mRNA	~2%	~2,500		
~2 nm	tRNA	~3%	~160,000		
~2 nm	RNA	~21%			
~4 nm	Globular Protein				
~10 nm (thickness)	Cell membranes	~10%		Use nanoneedles to pierce these membranes with minimal disruption to the cell.	To enhance drug/vaccine delivery of cells through perfusion.
~11 nm	Ribosome	~9%			
~25 nm	Microtubule diameter				
~75 nm (envelope thickness)	Endoplasmic reticulum (smooth, rough, Golgi)	~15%		Target with RNA, mRNA, iRNA for up regulating or interfering the production of proteins.	Vaccination, gene therapy for cancerous cells.
~100 nm	Large Virus				
~200-500 nm	Lysosomes	~1%		Pierce the lysosomes to	Inducing cell death in

				release enzymes and induce autolysis (self digestion of the cell).	cancerous cells.
~3 μm x 200 nm	Mitochondrion	~22%			
~3-6 μm	Nucleus	~6% (Liver) 16% (LC's)	1	Target for DNA delivery to the cell directly and/or disturb the double membrane.	DNA vaccination or gene therapy.
~10-30 μm (diameter)	Cell			Langerhans cells are ~10 μm in diameter.	

2. Routes Of Delivery To Cells

The type and scale of organelles within cells has been presented. Now the location of these cells within the tissue is identified. The selected tissue routes are.

- Intradermal
- Mucosal
- Lung
- Internal tissues
- In-vitro sites.

2.1 Intradermal Delivery

The skin is one convenient route for drug and vaccine delivery. A schematic of the skin is shown in Figure 6 with the corresponding structure shown schematically at a higher scale of resolution in Figure A.. A full description of the anatomy of the skin is given in textbooks. A closer view of a histology section of skin is shown in Figure 7

in a photomicrograph. Respective thicknesses of layers vary between species and sites.

A key barrier to many drugs and vaccines is the Stratum Corneum (SC). In humans, this barrier is 10-20 μm thick with large variations from site-to-site with different ages and sexes. Below the SC is the Viable Epidermis (VE), which is typically 40-60 μm thick in humans. Within the VE are immunologically sensitive Langerhans Cells (LC). Figure 7 shows a stained LC, marked as "L", residing above the basal layer. The spatial distribution of LCs is illustrated in a 3D distribution of LCs in a mouse, Figure 8 (Kendall M.A.F., Mulholland W.J., Tirlapur U.K., Arbuthnott E.S., and Armitage, M. (2003) "Targeted delivery of micro-particles to epithelial cells for immunotherapy and vaccines: an experimental and probabilistic study", The 6th International Conference on Cellular Engineering, Sydney, August 20-22).

There are typically about 1000 LCs per square mm and they reside just above the basement membrane of the viable epidermis (i.e. 30-80 μm deep). Importantly, the depth of LCs varies significantly with the biological variability of the tissue, including rete ridges etc.

One objective in vaccination and gene therapy applications is to target LC residing 30-80 μm below the skin surface. In order to do this, the SC and cell membranes are to be breached. Furthermore, the organelles within the LC are to be targeted to elicit particular responses. One example is in the triggering of MHC I responses, whereby intact DNA is to be delivered to cell the nucleus. Alternatively, mRNA can be delivered to the Endoplasmic Reticulum or the cytoplasm.

Similarly, in the treatment of skin cancers such as Squamous Cell Carcinoma, cancerous cells within the VE may be directly targeted.

In some applications it may be beneficial to target cells deeper into the dermis. For example, in Basal Cell Carcinoma, the cells to be targeted are deeper in the tissue, approaching hundreds of microns (600 μm± 800 μm) (British Journal of Dermatology 149(5) Page 1035 - 2003).

2.2 Mucosal Delivery

Fig. 9 shows a photomicrograph of a histology section of the mucosa. The physiology of the mucosa is similar to the skin. However there are some notable differences:

- the mucosa does not have a stratum corneum
- the epithelium is 600-800 μm thick. This is considerably deeper than the epidermis of the skin (the exact thickness varies with site, age and species).

Therefore, to target organelles within cells at the basement membrane of the epithelium, a depth of 600-800 μm is required.

2.3 Lung Delivery

The epithelial cells on the lining of the lung are the target for various gene therapy approaches. These cells are underneath a mucous/liquid lining, which may be 10-100 μm thick. Therefore this lining needs to be overcome. In the example of gene therapy for the treatment of Cystic Fibrosis, this lining is to be overcome to target celial cells on the surface of the epithelium.

2.4 Other Internal Organ Delivery

Cells within other the internal organs can also be targeted for a range of applications, such as:

- Internal cancers
- Liver (e.g. for Malaria treatment)
- Heart (e.g. for angiogenesis blood vessel formation).

2.5 In-vitro delivery

Tissue, cell-lines, tissue culture, excised organs, tissue engineered constructs and artificial tissues may also be targeted, in-vitro. Examples include:

- stimulation of cell lines and cell monolayers in culture.

- stimulation/delivery of growth factors and/or genes (e.g. in tissue engineering and wound healing).

3. Constructional features of the micro- nano projections.

3.1 General Micro-nanoprojection dimensions

With typical cell and organelle scales described and locations in tissues highlighted, the structural terms of the nanoneedles individually are described, and then as examples of arrays for targeting cells at different tissue sites.
Nanoneedles are configured to penetrate the cell membrane with minimal damage, targeting the organelles of interest. The overall dimensions of the nanoneedle projection are shown in Figure 10. The nanoneedle is divided into two main sections:

3.1.1 The cell/organelle targeting section, length (*l*)

Referring to Fig. 10, the radius of the tip (r) is to be as small as practicable with limits set by manufacturing methods and material considerations, where usually the diameter at the distal end of *l* is d_1. Usually d_1~2r. The diameter of the upper end of *l* is defined as d_2. Over the length *l*, the effective diameter, tapering from d_1 to d_2 is to be considerably less than the diameter of the cell (d_{cell}). It is shown in Table 1 approximately that 10 μm < d_{cell}< 30 μm. So, approximately, d_1<< 10 μm, preferably < 1 μm, ideally in some cases < 500 nm. Ideally, the scale of d_1 is to be of the order of the organelle of interest.

For practical engineering and manufacturing and purposes (e.g. buckling/loading/fracture) it is often preferred that the projection along *l* tapers out to a larger diameter (d_2>d_1) that still is less than the diameter of the cell (< d_{cell}). However, along the length of *l*, the profile may be configured such that the diameter is constant (i.e. d_1=d_2).

The length of the targeting section (*l*) is sufficient to ensure that the organelle of interest is targeted (i.e. *l* > organelle dimension). For example, in targeting the cell nucleus, *l* > 3-6 μm). Ideally, *l* is even longer to account for variation in cell depth

location (e.g. as shown by the variation in the Langerhans cell depth Figure A) and increase the probability of the desired needle-organelle contact. The upper length of *l* is determined by the combination of material properties, needle shape and loading to ensure that the needle does not break under mechanical loading. Engineering analyses shows this mechanical loading is mostly compression, with tension and bending moments. Good engineering practice to ensure the material does not break includes Euler buckling, fracture mechanics, and work-to-failure. In considering a population of projections in an array, statistical methods (e.g. Weibull statistics) and other related methods may be applied to ensure a very small fraction of the projection population breaks.

Consider, as an example, the case of compression loading with the primary mode of projection failure is by buckling. This compression buckling criteria set by the Euler Bucking force (P_{cr})

$$P_{cr} = \frac{\pi^2 EI}{4l^2}$$

where (E) is the Young's modulus of the nanoneedle material, I is the moment of inertia ($I = \frac{\pi d^4}{64}$ for a cylinder). Therefore the material properties of the nanoneedle and shape determine the maximum force permitted for buckling (P_{cr}). Good engineering practice dictates that P_{cr} must be less than the insertion force of the needle, to ensure it does not break.

3.1.2 Support section of the micro-nanoprojection (*a*)

Referring again to Fig. 10, the support section of the micro-nanoprojection (*a*) is sufficient to bring the targeting section of the cell (*l*) into contact with the cells/organelles of interest. The diameter of the support section along the length *a* tapers at the distal end from d_2 to d_3 at the base, where usually engineering and material considerations result in $d_3 > d_2$ to ensure it does not buckle or break by another mode of failure. In some cases, the diameter along the length of *a* may be constant

(i.e. $d_3=d_2$). Fig. 10 shows that a, l and the overall length of the projection (L) are related by:

$$L = a + l$$

In section 2 the depths of cells for various applications in intradermal, mucosal, lung and internal organ delivery are outlined. The rationale and approximate values of a for targeting these individual sites are presented as examples.

In epidermal delivery, a is the sum of the desired depth in the tissue and an allowance above the target (for instance for tissue surface curvature). This dimension in epidermal delivery is usually < 200 μm in length, and preferably < 100 μm in length—depending on the tissue species and site. In the targeting of dermal cells, this depth is even greater with a < 1000 μm, and preferably < 600 μm In another example, the targeting of basal cells in the epithelium of the mucosa, an a of 600-800 μm is required. In lung delivery, the local barrier of the mucous lining to the cells is 50-100 μm thus a would be of the order of 100 μm in this case.

3.2 Specific Applications

3.2.1 Example 1:

Targeting the nuclei of LCs in the viable epidermis, 40-50 μm deep in the tissue. The force to insert the needle is estimated with the Unified Penetration Model (proposed by Dehn J: A unified theory of penetration. International Journal of Impact Engineering, 5: 239–248. 1987).

$$F_{insert} \approx 3A\sigma_y = 3\frac{\pi}{4}d^2\sigma_y$$

where σ_y is the yield stress of the tissue. Assume, in the highest loading case, the upper value of the yield stress of the SC of 20 MPa applies to all the skin (from Wildnauer RH, Bothwell JW, Douglas AB: Stratum corneum properties I. Influence of relative humidity on normal and extracted stratum corneum. Journal of Investigative Dermatology, 56(1): 72–78. 1971). Note, this estimate of insertion force

is a factor of 10 greater than calculations inferred from measurements with a probe in the skin (unpublished results, by Crowley (2003, 4th Year Project, Engineering Science, University of Oxford).

By setting $F_{insert} = P_{cr}$ we arrive at

$$l = (\frac{\pi E d^2}{192\sigma_y})^{0.5}$$

which approximates the Euler Buckling relationship between the maximal permissible length of extension for a probe of diameter d, constructed of a material with a Young's modulus (E), penetrating into a tissue with a Yield Stress (σ_y).

Figure 11 plots the cell/organelle targeting section length (l) as a function of diameter for six materials. Note that these are upper limit calculations of the loading effects.

Consider the curve for titanium (E= 116 GPa) in which a 400 nm diameter (d_1=d_2) cell/organelle targeting section corresponds to a length of 7 μm, and a 1 μm diameter corresponds to a maximum length of 14.1 μm. In this case, the nucleus of the LC is the organelle of interest with a size of 3-6 μm. Here, we choose a organelle targeting section of d_1=d_2=1 μm and a length (l) of 10 μm (symbols corresponding to the diagram of Figure 10). The support length (a) is 40 μm, tapering to a base diameter (d_3) of 5 μm. These dimensions are summarised in Table 2.

Alternatively, a nanoneedle constructed of a stiffer material such as silicon (E=189 GPa) results in a smaller cell/organelle targeting section of d_1=d_2=200 nm over a length (l) of 5 μm. Of course, a brittle material such as silicon would also require fracture (and other) analyses that may lead to more conservative (i.e. larger) dimensions—these numbers throughout this section are simply illustrative.

Utility of an even stiffer material such as Tungsten (E=400 GPa) results in the same nanoneedle diameter of $d_1=d_2=200$ nm extended over a length (l) of >6 μm—or alternatively the possibility of a smaller diameter $d_1=d_2<200$ nm for a length of 5 μm.

3.2.2 Example 2

Targeting the Endoplasmic Reticulum LCs of the Viable Epidermis. Table 1 lists the thickness of the Endoplasmic Reticulum envelope to be 75 nm. Choosing titanium, the organelle targeting section is set at 400 nm over a length of 5 μm. As shown in Table 2, the remainder of the components are identical to those set out in Example 1.

3.2.3 Example 3

Targeting cell nuclei at a depth of 600 μm in the tissue. Here, the targeting section is identical to Example 1, whereas the considerably longer length (a=600 μm) requires a significantly wider base (d_3= 50 μm).

3.2.4 Example 4

Figure 10 shows an axi-symmetric design for the nanoneedle. Alternative shapes may be used with:

- higher values of mass-moment of inertia (I)
- more knife-like geometries with sharper leading edges.

One possible example of an alternative shape taking on these features is shown in plan view in Figure 18.

Table 2: The geometry of three nanoneedle examples.

Example	r (nm)	d_1 (nm)	d_2 (nm)	l (μm)	d_3 (μm)	a (μm)
1. Nucleus of LCs, 40-50 μm deep	< 1000	1000	1000	10	5	40
2. Endoplasmic Reticulum of LCs 40-50 μm deep	<400	400	400	5	5	45
3. Cell nuclei, 600 μm deep.	< 400	1000	1000	10	50	600

4. Route For Transfer Of Bioactive Material To End Point (Coating)

Consider the generic shape of the micro-nanoprojection (Fig 10). The bioactive material is coated to the outer surface of the micro-nanoprojection. The following lists two example protocols on how this is done, followed by a list of possible coating combinations.

4.1 Coating DNA on metallic (e.g. gold or tungsten) micro-nanoprojections

Consider the case of coating eGFP to tungsten micro-nanoprojections. Essentially, published and well established protocols devised for coating gold microcarriers for biolistic delivery are employed. Examples of these protocols are detailed in: PowderJect and Bio-Rad patents and protocols such as http://plantsciences.montana.edu/wheat-transformation/biolisti.htm); J.E. Biewenga, O.H. Destree, L.H. Schrama, "Plasmid-mediated gene transfer in neurons using the biolistics technique", J. Neurosci. Methods 71 (1997) 67–75; S. Novakovic, M. Knezevic, R. Golouh, B. Jezersek, "Transfection of mammalian cells by the methods of receptor mediated gene transfer and particle bombardment", J. Exp. Clin. Cancer Res. 18 (1999) 531–536; H. Wellmann, B. Kaltschmidt, C. Kaltschmidt, "Optimized protocol for biolistic transfection of brain slices and dissociated cultured neurons with a hand-held gene gun," J. Neurosci. Methods 92 (1999) 55–64; and , John O'Brien , Sarah C.R. Lummis "An improved method of preparing microcarriers for biolistic transfection", Brain Research Protocols 10 (2002) 12–15.

In this example, subsequently applied to the Experimental Exemplificaton 1 (section 5.3) the protocol of O'Brien and Lummis (2002) is applied.

Alternatively, in coating silicon, protocols developed for the sub-micron patterning of DNA oligonucleotides for "lab-on-a-chip" technology can be applied to coating the projections on the array (H. B. Yin, T. Brown, J. S. Wilkinson, R. W. Eason and T. Melvin (2004) "Submicron patterning of DNA oligonucleotides on silicon" Nucleic Acids Research, 2004, Vol. 32, No. 14 e118). This process is an example of two-stage process for the covalent attachment of DNA oligonucleotides onto crystalline silicon (100) surfaces. In summary, UV light exposure of a hydrogen-terminated silicon (100) surface coated with alkenes functionalized with N-hydroxysuccinimide ester groups result in the covalent attachment of the alkene as a monolayer on the surface. Submicron-scale patterning of surfaces is achieved by illumination with an interference pattern obtained by the transmission of 248 nm excimer laser light through a phase mask. The N-hydroxysuccinimide ester surface act as a template for the subsequent covalent attachment of aminohexyl-modified DNA oligonucleotides. Oligonucleotide patterns, with feature sizes of 500 nm, are reliably produced over large areas. The patterned surfaces are characterized with atomic force microscopy, scanning electron microscopy, epifluorescence microscopy and ellipsometry. Complementary oligonucleotides are hybridized to the surface-attached oligonucleotides with a density of ~7 x 10^{12} DNA oligonucleotides per square centimeter (for example).

Some possible coating combinations include:

- No coating: The cell is perturbed/stimulated by the physical disruption of the micro-nanoprojection structure. This physical stimulus can be coupled with electric stimulus as a form of specific nanoelectroporation of particular organelles or the cell.
- Coating entire nanoneedles: The bioactive material can coat the whole surface of the nanoneedle (over the length L).
- Selective coating: For certain applications only parts of the nanoneedle need be coated. For instance, the targeting section (l) can be selectively coated by only immersing this part of the needle in the coating media. Alternatively, different

combinations of various coatings can be made on the one nanoneedle (combinations of DNA and adjuvants, proteins, cytokines, inhibitors etc). Or, in the case of nanoneedle arrays, different coatings may be provided on different individual micro-nanoprojections.

- Coating materials: In addition to bioactive materials (such as DNA, RNA and proteins), the micro-nanoprojections may also be coated with nanobiosensors (e.g. quantum dots, nanomachines, MEMS) using a range of coating protocols.
- Material formulated in degradable micro-nanoprojections: All, or part of the micro-nanoprojection can be constructed of a biocompatible, biodegradable polymer (such as Poly Lactic Acid (PLA), Poly Glucleic Acid (PGA) or PGLA), which is formulated with the bioactive material of choice. The micro-nanoprojections may then be inserted and, as they dissolve, the bioactive material will enter the organelle(s)/cells.

In the cases of bonding of the biomaterials to the surface of the micro-nanoprojections, access to the organelles may be by the following:

- The bioactive material can stay on the surface of the nanoneedle, but elicit the response within the organelle/cell.
- The bioactive material bonds can be broken by exposure of enzymes, proteins or hydration within the cell/organelle.

5. Experimental Exemplification 1

This section outlines the simplest embodiment of the nanoneedle concept: an individual projection, coated on the surface with a bioactive material (here DNA coded for GFP transfection), used to deliver this material to a living cell, in-vitro, where a biological response is measured (transfection) and the cell is alive.

5.1 Fabrication of micro-nanoprojection.

Following the engineering analyses discussed in section 3, Tungsten was selected as the material for fabricating the individual nanoprojection, largely because of its high stiffness (E= 400 GPa) and ease of fabrication.

Individual micro-nano projections were fabricated from tungsten rod of diameter 280 μm (Source, ADVENT Research Materials Ltd) using electropolishing

(approximately following the protocol of Cerezo, A., Larson D.J. & Smith G.D.W. (2001) "Progress in the atomic-scale analysis of materials with the three-dimensional atom probe". *Materials Research Society Bulletin*, 26(2):102–107.

A photograph of the electropolishing set-up is shown in Fig. 12, with the electrical leads connected to a A/C power supply (not shown). The solution in the beaker was distilled water with 4% NaOH molar. For the electropolishing tungsten probes with the sharpest tips, the following settings were used:

- 3mm of probe submersed into the solution
- 10 volts A.C. for approx. 42 seconds

Following optimisation, electropolishing was ceased when probe length began to diminish (detected by visual sighting by naked human eye).

5.2 Example of individual electropolished projections.

Recall the dimension parameters correspond to the generic micro-nanoprojection tip outlined in the schematic of Fig. 10.

Fig. 13 shows Transmission Electron Microscopy (TEM) of an electropolished Tungsten tip at two different resolutions, with the scale bar in (a) of 20 μm, and in (b) of 0.11 μm. Fig. 13(b) shows the minimum tip size (d_1) is ~100 nm (i.e. r~50 nm). By using the electropolishing process, the projection gradually tapers to the full thickness of the original rod (i.e. d_3=280 μm) . In this case, the cell targeting length (l) is approximately 20 μm—defined by where the diameter (d_2) remains less than ~1 μm.

Individual micro-nano projections were glued into hole drilled into perpex cylindrical holders to allow fitting into microprojection systems (see section 5.5).

5.3 Coating of micro-nanoprojections with eGFP DNA plasmid.

The tungsten micro-nanoprojections were coated by adapting a protocol devised for the coating of gold microparticles for biolistic delivery developed by O'Brien and Lummis (2002) "An improved method of preparing microcarriers for biolistic

transfection", Brain Research Protocols 10 (2002) 12–15. The adapted protocol is as follows:

(i) Coat tungsten micro-nanoprojection in 50%glycerol/50% water solution by dipping the wire in the solution for 10 minutes.

(ii) Remove the tungsten.

(iii) Individual tungsten micro-nanoprojections were placed in a tube to which was added 50 ml of 1 M spermidine for 5 minutes.

(iv) Add 1 μg/ml of 50 ml of DNA Spermidine and gently mix the two solutions with aspiration with the wire in the solution.

(v) Gently, the tube was stirred for a few minutes, and then, whilst stirring, 1 M CaCl in solution was added in a drop wise manner.

(vi) Gently mix the solution and let DNA precipitate on to the wire for 30 minutes.

(vii) Remove wire from solution and dip it in 100% ethanol. Repeat this process 3times.

(viii) Let the wire dry before use.

(ix) The process was then repeated for the other micro-nanoprojections.

Fig. 14 shows images of lengths of tungsten wire (280 μm diameter) imaged with a fluorescent microscope with (a) uncoated wire and (b) DNA coated wire (using the described protocol, above) immersed in a liquid with a propidium iodide stain (red fluorescing dye). As expected there is no red fluorescence with the uncoated wire, while the strong red fluorescence of the NDA coated tungsten qualitatively shows that the coating was successful.

5.4 Assessment of delivery into in-vitro test bed.

To assess the delivery profile of DNA in the in-vitro equivalent of skin tissue, DNA coated projections were inserted into an agar (3%) gel stained with acridine orange (green fluorescing dye). This gel (without the stain) is routinely used for in-vitro testing of biolistic devices for DNA vaccination and other applications.

The uncoated and coated tungsten rods were inserted and removed by hand into the agar (to a depth > 1 mm) for a cycle duration of approximately 1 second.

Fig. 15 shows optically sectioned Multi-Photon Microscopy (MPM) images of the agar after insertion of a DNA coated tungsten probe (a) on the surface (b) at a depth of 13 μm (c) at a depth of (32 μm). Also shown in (d) is an optical section at 32 μm of agar gel following insertion of a probe without a DNA coating.

On the surface of the agar, there is very little fluorescence, indicating little DNA. In contrast, at depth sections of 13 μm and 32 μm the fluorescence in the coated case is significant—indicating that DNA remained intact on the surface of the probe during insertion and then came off by exposure of the gel and/or by the action of removing the probe. This fluorescent signal was very strong compared with the uncoated probe control at 32 μm.

5.5 Experiment of DNA delivery into a cell.

The described electropolished tungsten micro-nanoprojections coated with GFP plasmid DNA were tested, with the objective of determining whether the DNA could be delivered to transfect the cell, without damaging the cell.

The cell line is called A549 which is a human lung carcinoma (epithelial) cell line. Cells were cultured in Dulbecco's modified eagle medium (DMEM) supplemented with 10 % fetal calf serum at 37°C, 5% CO_2.

These cells were mounted on three separate Petri dishes with an optical slide underneath. The adherent properties of the cells ensured they remained in contact with the base of the dish.

One of the Petri dishes with cells was set aside as a control. The other two Petri dishes were probed with the micro-nanoprojections. In total, 6 micro-nanoprojection systems were used.

Probing of the cells was performed with a microinjection system (Eppendorf Femtoject and Injectman NI2 microinjection kit) fitted to an inverted fluorescent microscope (Zeiss Axiovert 25 microscope with stage heater).

The micro-nanoprojection were fitted into the standard microinjection holder and then moved with course and fine adjustment of a motorized X-Y-Z axis controller to just contact the cell membrane, before retraction of less than 1 μm.

A cycle time of probing was set between limits of 0.1 and 15 seconds, with a traverse distance of 3-5 μm—then the cycle was automatically performed on the system. After 3 cells, the probe was replaced and refitted with a replacement. In total 10 cells were perturbed with a micro-nanoprojection coated in eGFP plasmid DNA.

All the cell samples were then incubated for 24 hours before viewing with a widefield fluorescent microscope, with the appropriate fluorescent filters. The observed results show: in the control there is no sign of eGFP transfection, as expected. However, in the cell micro-nanoprojection cases, we see that 10 cells have transfected. Thus we have a 100% transfection efficiency and no evidence of cell death.
These data prove the micro-nanoprojections, coated in DNA can individually target cells, transfecting them and not kill them.

Also, subsequent analysis of the micro-nanoprojections showed they remained intact, illustrating that unlike biolistic delivery, the "carrier" material is not left behind.

6. Experimental Exemplification 2:

With the biological result achieved on a single cell, in-vitro (Experimental exemplification 1). this section outlines a logical progression, which is the physical testing of an individual micro-nano projection into a representative skin sample for structural integrity—thereby testing the engineering analyses outlined in section 3.

6.1 Experiment design

Using the electroporation process described in Embodiment 1, a micro-nanoproprojection was fabricated of Tungsten with a tip radius (r) of <400 nm.
The tissue was freshly excised Balb/C mice ears (age 8-10 weeks), which were glued to a metal cylinder holder. The reported stratum corneum and viable epidermis thicknesses of these samples are respectively ~5μm and 12 μm (Arbuthnott (2003)).

The tissue was indented by fitting the micro-nanoprojection to a Nanoindenter (MTS systems, UK), measuring a force displacement curve. Fig. 17 shows two typical sample results of loading-unloading curves achieved to a depth of ~50 μm. These results show that the micro-nanoprojection probe penetrated through the epidermis and well into the dermis without damage. The difference in magnitude between the curves is typical of biological variability observed in bio-viscoelastic tissue. Importantly, unlike ballistic particle delivery, the depth of penetration is not dependant upon this variability—rather the length of projection.

Indeed, the projections did not break—the loading experiment was simply stopped at a 50 μm setting on the experimental apparatus. This was confirmed by imaging with projections with a microscope after the experiment. This experiment was repeated 20 times, confirming the engineering analyses of probe structure required to target cells in the skin is applicable and valid.

6. Experimental Exemplification 3: Overall Size Range Of Individual Patch

With the biological and engineering criteria investigated on an individual projection, the next logical step is to extend the concept to arrays of patches targeting tissue sites. Presented are several patch arrangements, each designed for a particular targeting need of cells, organelles and/or tissue sites.

6.1 General Dimensions and design of patch

Figure 19 shows a schematic of an array of the described micro-nanoprojections configured on a patch, with the spacing between micro-nanoprojections defined as (S) and the patch breadth defined as (B). Recall, the basic dimensions and definitions of an individual micro-nanoprojection are outlined in section 3 and shown schematically in Fig. 10; these are referred to again here.

Operation of the patch with the micro-nanoprojections is, for example:

(a) the slow insertion, by hand (or other means, such as a spring) of the patch onto the tissue, with the micro-nanoprojections inserting into the target tissue of interest.

(b) the patch including the micro-nanoprojections are held in place for a sufficient time for the "event" (biological, physical or other) to take place. This may be instantaneous, or in other cases could take days, weeks or months.

(c) the patch including the micro-nanoprojections are then retracted.

These three stages form a cycle, that may be operated by hand or automated with the aid of suitable mechanical, electrical or electro-mechanical devices.

Patches may be applied to the tissue site once, or a multitude of times depending upon the effect desired.

The case examples presented in 6.2 all centre on the targeting of Langerhans cells or organelles within these cells and the overall dimensions of the individual micro-nanoprojections are configured, using the approximate guideline of Example 1 and 2 shown in Table 2. However, as Table 2 also shows, these parameters (r, d_1, d_2, l, d_3, a) can vary significantly, depending on the cell/organelle and its position relative to the tissue surface.

6.2 Case examples of patch configurations

The overall size (BxB) of the patch and spacing (S) between the micro-nanoprojections is determined by the application. Note, in all cases, the patch could be square (BxB), circular, elliptic, or any other suitable shape. For simplicity, the square dimensions are quoted throughout. Generally the size is to be less than 15x15 mm (B), with $1<S<1000$ μm, preferably with $10<S<200$ μm.

Note that an alternative for these and other patch examples is for larger patches, giving amplified responses and/or which may be easier to handle having regard to end users/patients/practitioners.

6.2.1 Targeting LC Nuclei

Consider Example 1 from Table 2, which is the targeting of nuclei of Langerhans cells. Kendall et al. (2003);, Kendall M.A.F., Mulholland W.J., Tirlapur U.K., Arbuthnott E.S., and Armitage, M. "Targeted delivery of micro-particles to epithelial cells for immunotherapy and vaccines: an experimental and probabilistic study", The

6th International Conference on Cellular Engineering, Sydney, August 20-22), suggest that to trigger cellular responses in DNA vaccination, of the order of 100 nuclei of LCs are effectively transfected in gene gun applications that lead to the desired cellular (MHC 1) systemic response. A probability analysis has been performed to determine the configuration of patch required to transfect 100 cells. The probability of one micro-nanoprojection making contact with an organelle (or cell) defined over an area and volume is set by:

$$P_{contact} = \frac{V_{probe}}{V_{layer}} \cdot \frac{V_{organelles}}{V_{layer}}$$

In the analysis, it is assumed:

- that there is no cell death.
- the cell/organelle targeting sections (l) are configured to be at the correct depth (i.e. the depth of the Langerhans cells), and, for simplicity, parallel and 1 μm in diameter (d_1=d_2=1 μm).
- the cell/organelle targeting sections (l) are coated in DNA. Of course, for simplicity of coating, it is possible that most or all of the micro-nanoprojection structure is coated in DNA.
- contact of any part of the micro-nanoprojection along the cell/organelle targeting section with the nucleus is the only mode that leads to transfection (i.e. cytoplasm delivery, cross-priming and other modes are ignored).

With a 1 μm diameter cell/organelle targeting section (l), the probability of contact with a LC nucleus is 0.0131. This probability is ~1000-1500 times higher than a typical probability of a direct "hit" with the biolistics approach and microparticles. Furthermore, the transfection comparison is even more favourable for the micro-nanoprojection patch, given far fewer cells are killed than by the gene gun.

Table 3 is a summary of configurations of patches that may be used. At one end of the range, a spacing of 100 rods/mm^2 corresponds to a patch surface area of 76 mm^2, with a spacing (S) of 100 μm, a breadth of 8.7 mm and a total number of rods of over

7000. Increasing density of rods to 1000 /mm^2 results in a reduction in patch size to less than 3 mmx3mm.

Table 3: Calculated patch configurations for the targeting of nuclei of LCs.

Rod/mm^2	Area of patch (mm^2)	Spacing (S) (μm)	Breadth of patch (B) (μm)	Total Rods
100	76.4	100	8.7	7639
500	15.3	45	3.9	7639
1000	7.6	32	2.8	7639

6.2.2 Targeting the LC

In Table 4, this analysis is extended to the configuration of patch required to target 100 LCs (i.e. anywhere within the complete cell), using micro-nanoprojections with the same geometry as above, with the probability of the event 0.063. Not surprisingly, this is higher than the probability of targeting the nuclei. Hence, less rods are needed and the patch size can be smaller (4x4 mm down to 1.25x1.25 mm).

Table 4: Calculated patch configurations for the targeting of anywhere within complete LCs. The nanoneedle diameter d_1 is assumed to be 1 μm.

Rod/mm^2	Area of patch (mm^2)	Spacing (S) (μm)	Breadth of patch (B) (μm)	Total Rods
100	15.8	100	4.0	1578
500	3.2	45	1.8	1578
1000	1.5	32	1.3	1578

6.2.3 Targeting the Endoplasmic Reticulum of the LC.

In Table 5, the analysis is also applied to the targeting of the Endoplasmic Reticulum (Example 2 from Table 2), which may be required for targeted RNA delivery. Using the assumptions from above, with a probe diameter of 400 nm the probability of a

single needle contacting the Endoplasmic Reticulum is 0.031. In this case, the size of patch ranges from 8x8 mm to 2.5x2.5 mm.

Table 5: Calculated patch configurations for the targeting of the Endoplasmic Reticulum of LCs. The nanoneedle diameter is assumed to be 400 nm.

Rod/mm^2	**Area of patch (mm^2)**	**Spacing (S) (μm)**	**Breadth of patch (B) (μm)**	**Total Rods**
100	65	100	8.0	6451
500	13	45	3.60	6451
1000	6.5	32	2.54	6451

6.2.4 A combination of micro-nanoprojection geometries on a patch.

A patch may also have combinations of micro-nanoprojections, with different geometries. For example the length (*L*) or indeed the other parameters in Fig. 10 may be varied throughout the patch, either in defined sequences, clusters and/or randomly (within limits). Within this, or separately, the diameter of the projection may be increased on individual micro-nanoprojections significantly in order to induce cell death at controlled locations. This, for example, may be used to induce bystander biological responses (e.g. stimulation/inflammation/activation) to neighbouring healthy cells—which could have or will be interacting with described, smaller micro-nanoprojections configured for minimal cell damage.

7. Specific Bioactives e.g. Nucleic Acids

The bioactive or other stimulus is to be coated or part of the nanoneedle array. The choice of bioactive is determined by the application and target organelles or cells of interest. This range encompasses, but is not restricted to:

- No coating
- Polynucleotides, DNA (all variants), RNA (all variants), proteins, antigens, allergens and adjuvants, molecules, compounds.
- Biosensor molecules and compounds and materials.
- Nanosensors (MEMS etc).
- Combinations of the above, on a

8. Methods Of Production Of Device

General requirements of the manufacturing method are:

- a radial resolution of <200 nm;
- to construct the nanoneedle array on a patch (e.g. Fig 19) in a scaleable process for high throughput manufacturing with minimal human input.
- Construction to be of a medical grade material (e.g. Gold, Silver, Titanium, Tungsten or PLA, PGA, PGLA, Silicon)

A range of techniques for micro-nanofabrication methods described in text books, papers and in other literature (e.g. Madou M.J. "Fundamentals of Microfabrication. The science of miniaturization", CRC Press, 2002; McAllister et al. 2003, PNAS, Nov 25, 2003, Vol 100, number 4) are applicable to the nanoneedle device here.

Furthermore there are a range of materials and fabrication methods being developed that also have potential utility as part of a micro-nanoprojection array. Three construction embodiments are shown here as examples.

In these constructional embodiment example cases, the patch geometry of manufacture is summarised in Table 3, with an area of patch ~76.4 mm^2, a spacing of 100 μm and the minimum tip size of 1 μm (d_1). A schematic of this array on patch is shown in Fig. 20. Of course, the techniques can be applied to a range of geometries.

8.1 Constructional embodiment example 1:

As an example of the fabrication of silicon micro-nanoprojections, the following is applied. Deep Reactive Ion Etching (DRIE) is used as a process ideal for these high aspect ratio structures, where in one example (Oxford Instruments Plasmalab System 100, Modular ICP180 Etch System-S12), etch rates of > 2.5 μm/min, and sometimes >5 μm/min, are possible. Full details of etch protocols for this system are available in the literature, including Oxford Instruments company manuals.

Briefly, chromium was sputter deposited then lithographically patterned as an array of dots onto 3 inch (75 mm) 100 oriented silicon wafers. The array of dots had a centre-

to-centre spacing of 100 μm, and in some earlier test cases, 10-20 μm. Similarly, through iteration with the conditions and exploring the extent of undercut, the diameter of the dots 1 μm, and in other cases, 3μm, 5 μm, and 10 μm.
Deep Reactive Ion Etching (DRIE, Oxford Instruments, Bristol, UK) was then carried out to obtain the desired by profile by adjusting the etch rate. The typical instrument conditions included a 20 standard cm^3/min (sccm) SF_6 and 15 sccm (O_2) at a pressure of 20 Pa. Power was varied. The etching process was performed at cryo-cooled conditions, achieving temperatures of -100 to -150°C. Lower etch rates were used for the tapered sections, whereas higher rates were used for the more parallel sections. Micro-nanoprojection fabrication was finished when the chromium masks became fully undercut and fell off the projection tips. The process is completed in less than 100 minutes, resulting in several patch configurations on the wafer.
The patches were then cut from the silicon wafer, with a dedicated cutter.

To increase the strength of the base of the patch, an additional, thicker material is affixed to the back surface (i.e. the surface *without* the projections).

This process is repeated to fabricate a large quantity of micro-nanoprojection array patches.

A variation of the described DRIE method may also be applied to other materials, including Silicon Carbide (SiC).

8.2 Constructional embodiment Example 2:
This constructional embodiment example applies to a broader range of micro-nanoprojections materials than those described in the constructional embodiment Example 1. These materials include Metals, polymers, silicon and oxides/carbides.
As an example, this case illustrates a method of fabricating tungsten micro-nanoprojection arrays on a patch. Three of the steps in this production process are discussed.

Step 1: Construction of a Template (Male)
To construct a male template with the profile of the micro-nanoprojections, LIGA is used (a German acronym for X-ray lithography, electrodeposition and molding). This

template will serve in the production of several molds in a soft polymer. LIGA, which utilizes a Synchroton, is ideal for creating the template because it has a very high resolution (< 20 nm), can fabricate in metals, and will easily fabricate a patch (maximum component size is 3.4 inches in the Axsun technologies system). Fabrication protocols to construct the template are detailed in Chapter 6 of Madou M.J. "Fundamentals of Microfabrication. The science of miniaturization", CRC Press, 2002 manuals and literature from companies (e.g. AXSUN Technologies, Ca, USA). The choice of materials for fabrication include Nickel (Ni), Nickel-Iron (Ni-Fe), Nickel-Cobalt (Ni-Co) Gold, Copper and Silver. In this example, Nickel is selected as the material from which the micro-nanoprojection array template is constructed.

It should be noted here that as an alternative, LIGA could be used to make individual patches directly (e.g. of gold or silver—which are both biocompatible) in large quantities. With current costs of the LIGA technology, this is not practical—but with LIGA technology advances, this could be feasible in the future.

Step 2: Construction of a Mask (Female component)

Because of the discussed current characteristics of LIGA (e.g. cost), LIGA is not used to mass-fabricate micro-nanoprojection array patches for direct use with the tissue in large numbers. However, here it can be used as a template for many multi-stage processes. As one examples, the template is used for multiple insertions into a soft polymer to produce a mask, as shown in Figure 21, performed in the following steps:

- Fig 21 (A) Insertion of the template directly into the soft polymer. This is repeated several times to produce many indentations in the polymer with a given mask.
- Fig 21 (B) Allowing the soft polymer to harden, or "cure" with the addition of catalysts and or temperature.
- Fig 21 (C) Remove the template to leave behind a mask.

Step 3: Final Construction of the nanoneedle array with the mask

The masks are then be placed in a vacuum chamber and deposited with a vacuum deposition/sputtering process. The material to be sputtered is a biocompatible inert material, such as titanium, gold, or silver. In this process, the polymer surface is

treated with an air discharge before the chamber is pumped down to a vacuum at 27 degrees C. The titanium, gold or silver film is then deposited. Commercial sputtering machines may be used in this process (such as the Varian VM8 Sputterer).

If a charge is required to produce an anode to enhance the coating of the nanoneedle section, then the end extension of this piece can be "opened up" to expose a stronger anode which the positive charged metallic ions in solution are attracted to. This technique makes use of Magnetron Sputtering.

Step 4: Constructional embodiment Example 3 Method

The mask can then be removed by immersion of a liquid (e.g. alcohols) to dissolve it.

8.3 Constructional embodiment example 3:

Alternatively, a mask (female) can be directly manufactured using Two-Photon Stereo Lithography (2PSL), in which the geometry co-ordinates shown in Figure 21 (C) are applied to construct the desired shape with the photosensitive resin.

Femtosectond two-photon stereo-lithography (2PSL) is described in detail by Miwa et al. (2001, Appl Physics. A 73, 561-566). Zhou et al. (2002, Vol 296, Science), Stellacci et al. (2002, Adv. Mater. 14(3)) and Halik et al. (2003, Chem Commun. 1490-1491). This approach has demonstrated the ability to construct complicated 3D shapes with a resolution of <200 nm out of materials including photosensitive polymer resins and metals in conjunction with dyes. Lattice structures of the desired scale have been constructed with the technique using resins impregnated with Silver (from Stellacci et al. 2002).

Briefly, the technique works by scanning with a femtosecond laser in a liquid photosensitive resin bath. The two-photon effect ensures that solidification occurs only where the energy of the laser is concentrated to a femtolitre volume (typically 200 nm x 200 nm x 400 nm, x, y, z). The method of manufacture is to start at the tip of the nanoneedle (marked A in Figure 20) and then work up the needle to the base. The same approach applies to the rest of the nanoneedles. The process is fully automated with a motorised x-y stage with the laser co-ordinates determined from engineering drawings of the structure. Therefore, thousands of nanoneedles can be constructed in a scaleable process. The technique allows complicated 3D structures to

be constructed by the scanning of a pulsed (80 MHz), femtosecond pulse length laser concentrating light at 400-1000 nm to a femtolitre volume to induce a two photon excitation of the material and induce solidification.

The nanoneedles may be constructed with a photosensitive polymer/resin, (such as the commercial grade SCR 500) or an alternative impregnated with Silver (following Stellacci et al. 2002).

These materials are currently not suited to be used directly in the skin, due to:

- insufficient stiffness. Young's Modulus of SCR 500 is 0.49 Gpa compared with 116 Gpa for Titanium or 77.2 Gpa for Gold.
- Not medical grade material. At the time of writing, photosensitive resins such as SCR 500 had not gained approval for medical grade purposes.

However, the technique is rapidly improving and may be a possible fabrication method in the future.

8.4 Constructional embodiment example 4:

In this case nanoneedles are constructed with silicon, with a 200 nm tip for a length of 5 μm followed by two other parallel sections separated by tapered sections. This structure may be constructed by Electron Beam Lithography and Reactive Ion Etching, a standard technique in the microelectronics industry. The manufacturing approach has been applied by Henry et al. (Journal of Pharmaceutical Sciences 87(8), 1998) and in Lebouitz and Pisano et al. (US Patent 5928207) in the construction of microneeedles.

Fig. 22 shows the structure produced with one of these techniques. In this case of the nanoneedles, each parallel section may be constructed with silicon 100 wafers and the tapered sections constructed with silicon 111 (or other) wafer material—where the angle of the taper is a preferred etching line of the material. The shown shape is made from 5 wafers (one wafer per geometry). A gradual taper mould can be constructed from the one silicon wafer.

Alternatively, the silicon arrays may be used as masters for microarray moulds.

9. Methods Of Treatment

Recall in section 1 the specific target sites of key cells and organelles are described, followed in section 2 by their location within many tissue and in-vitro sites. With the described approach of targeting individual cells, then several cells and the shape/coating/fabrication considerations outlined, the methods of applying these micro-nanoprojection arrays to various tissue sites are now discussed.

9.1 Intradermal application.

With the described embodiments for the skin previously described, the patch is inserted into the skin either by user control or by mechanical, electrical or other controlled means. All these options are possible, as the magnitude of the forces is low. For example, the insertion force is approximately calculated to be less than 1 N (based on 7000 probes, 1 μm in diameter piercing tissue with a yield of 20 MPa). Similarly, the time of insertion, residence and removal from the tissue can be controlled by user and/or the described mechanical/electrical means.

One embodiment of a simple application system for the patch is shown in Fig. 23. In the retracted position (Fig. 23 a) the micro-nanoprojections patch is recessed and thus protected, preventing accidental administration. Other packaging/devices may also be used for these purposes, for example a protective cap to be removed before administration. In this example, the patch is attached to a compressed spring that is held in place by a tensioned string. When located on the tissue, the string is released by a means (e.g. pressing a button, not shown in Fig. 23) and the patch is released to enter the tissue surface (Fig. 23b).

9.2 Mucosal application.

To effectively target mucosal sites (e.g. mouth, nasal, rectal, vaginal), the described patch arrangements are fitted to an applicator designed to safely transport the patch into the mouth and to accurately locate on to the mucosal site. This could be done by using the described intradermal patch in the mouth. Alternatively, Fig. 24 shows one example of and applicator for mucosal delivery for the buccal mucosa (mouth). In this example, the patch arrangement from Fig. 23 is used, with the spring

arrangement—but others equally could be used. The applicator could have a button at the distal end from the patch to allow the operator to release the patch onto the mucosal site.

Other features may include a knurled surface towards the distal end to aid user grip.

9.3 Lower airway/Lung application

Fig. 25 shows a schematic of the physiology of the airways in a human. To apply the micro-nanoprojections to targeting cells in the tracheal or lung lining, an applicator that can flexibly and compactly reach these sites, target the sites, and then retract, is required.

As one example, Fig. 26 shows a deployable structure embodiment for targeting these sites. The method of operation is as follows. The flexible structure (Fig. 26(a)) is guided through the throat to the site of interest. This device may be fitted with imaging/illumination systems to help guidance. Fig. 26(b) shows the system in location in a "retracted" position. The arms fitted with the patches are held in place against a spring load with pivot points. Then, by mechanical actuation, the arms are released (Fig. 26(c)), with the springs providing the force for location on the tissue. The device does not need to be exactly centralised as the arms are self-locating. By tension with wires, the arms are retracted, and the device is removed through the throat.

In another embodiment, the arms are replaced by an inflatable structure (a "sock") fully coated by the micro-nanoprojections on the outside surface. When deflated, this sock would be held in a structure which would look similar to Fig. 26(a) on the outside. When in place, the sock would be inflated via a pressurised gas, locating on the tissue wall. This approach would be particularly useful where large surfaces need targeting, such as the lung. At the required time, the pressure is released with a valving arrangement and the sock collapses back into flexible targeting system and the device is removed.

9.4 Other internal tissues.

Other internal organs or tissues (e.g. liver, kidney, heart) are not as readily accessed as those described above. Here, more invasive means are required to expose the site of interest before targeting. One example is a more compact "catheter" version of the described lower airway/lung targeting devices, reaching the site via keyhole routes.

Another embodiment is surgery to fully open the site before application with the patch.

9.5 In-vitro sites.

The micro-nanoprojections may be fitted to patches for in-vitro targeting, allowing a high-throughput targeting of cells. In one example, larger patches with thousands and perhaps millions of projections could be mechanically lowered onto cell monolayers, and then removed, similar to a mechanical "press" arrangement. This could, for instance, allow a mass transfection of cells, in-vitro.

As another variation, cells are dynamically moving in a shallow fluid stream. As these cells move, they pass below large plates with thousands, and perhaps millions of micro-nanoprojections. These plates pressing into this cell layer repeatably, in a synchronised manner so that each pressing cycle targets the appropriate batch of cells.

CLAIMS

1. A device for the delivery of a bioactive material or other stimulus to an internal site in the body, comprising a plurality of projections which can penetrate a body surface so as to deliver the bioactive material or stimulus to the required site, wherein the projections are solid and the delivery end section of the projection is so dimensioned as to be capable of insertion into targeted cells to deliver the bioactive material or stimulus without appreciable damage to the targeted cells or specific sites therein.

2. A device according to claim 1, suitable for intracellular delivery.

3. A device according to claim 2, suitable for delivery to specific organelles within cells.

4. A device according to claim 1, suitable for delivery to a cell nucleus, endoplasmic reticulum, ribosome, or lysosome.

5. A device according to any of claims 1 to 4, wherein the projections comprise a support section of sufficient length to reach the desired site and a delivery end section having a length no greater than 20 microns and a maximum width no greater than 5 microns.

6. A device according to claim 5, wherein the delivery end section has a maximum width no greater than 2 microns.

7. A device according to claim 6, in which the maximum width of the delivery end section is no greater than 1000 nm.

8. A device according to claim 7, in which the maximum width of the delivery end section is no greater than 500 nm.

9. A device according to any of claims 1 to 8, for delivery intradermally.

10. A device according to claim 9, wherein the projections comprise a support section of length at least 10 microns and a delivery end section having a length no greater than 20 microns and a maximum width no greater than 5 microns.

11. A device according to claim 10, wherein the delivery end section has a maximum width no greater than 2 microns.

12. A device according to claim 11, in which the width of the delivery end section is no greater than 1000 nm.

13. A device according to claim 12, in which the width of the delivery end section is no greater than 500 nm.

14. A device according to any of claims 1 to 8, for mucosal delivery.

15. A device according to claim 14, wherein the projections comprise a support section of length at least 100 microns and a delivery end section having a length no greater than 20 microns and a maximum width no greater than 5 microns.

16. A device according to claim 15, wherein the delivery end section has a maximum width no greater than 2 microns.

17. A device according to claim 16, in which the width of the delivery end section is no greater than 1000 nm.

18. A device according to claim 17, in which the width of the delivery end section is no greater than 500 nm.

19. A device according to any of claims 1 to 8, for delivery to lung or other internal organ or tissue.

20. A device according to any of claims 1 to 8, for in-vitro delivery to tissue, cell cultures, cell lines, organs, artificial tissues and tissue engineered products.

21. A device according to claim 19 or 20 wherein the projections comprise a support section of length at least 5 microns and a delivery end section having a length no greater than 20 microns and a maximum width no greater than 5 microns.

22. A device according to claim 21, wherein the delivery end section has a maximum width no greater than 2 microns.

23. A device according to claim 22, in which the width of the delivery end section is no greater than 1000 nm.

24. A device according to claim 23, in which the width of the delivery end section is no greater than 500 nm.

25. A device according to any of the preceding claims, in which the delivery end section and support section is coated with a bioactive material across the whole or part of its length.

26. A device according to claim 25, in which the delivery end section and support section is coated on selective areas thereof.

27. A device according to any of claims 1 to 25, in which a bioactive material is releasably incorporated into the material of which the projection is composed.

28. A device according to claim 27, in which at least the delivery end section of the projection is composed of a biodegradable material.

29. A device according to any of the preceding claims, in which the bioactive material is a nucleic acid or protein.

30. A device according to any of the preceding claims in which the bioactive material is an antigen, allergen, or adjuvant.

31. A device according to any of the preceding claims in which the coating comprises molecules, elements or compounds.

32. A device according to any preceding claim, in which the coated material is a biosensor, nanosensor or MEMS.

33. A device according to any of claims 1 to 24, in which each projection has no bioactive material on or within it.

34. A device according to any of the preceding claims, in the form of a patch containing a plurality of projections for application to a body surface.

35. A device according to claim 34, in which the patch has at least 10 projections per mm^2.

36. A device according to claim 35, in which the patch has at least 100 projections per mm^2.

37. A device according to any of the preceding claims, constructed from biocompatible metals such as Titanium, Gold, Silver or tungsten.

38. A device according to claim 37, which is manufactured from a male template constructed with X-ray lithography, electrodeposition and molding (LIGA).

39. A device according to claim 38, where the template is multiply inserted into a soft polymer to produce a plurality of masks, which are then vacuum deposited/sputtered/magnetron sputtered with the material of choice for the projections.

40. A device according to claim 37, manufactured from a mask constructed with 2 Photon Stereolithography with the metal deposited using vacuum deposition, sputtering or Magnetron sputtering.

41. A device according to any of claims 1-36, constructed of silicon.

42. A device according to claim 41, manufactured with Deep Reactive Ion Etching (DRIE) from silicon wafers.

43. A device according to claim 37, manufactured with multiwafered Electron Beam Lithography.

44. A device according to any of claims 34 to 36 wherein at least some of the projections are of differing lengths and/or thicknesses to allow targeting of different targets within the same use of the device.

45. Use of a device according to any preceding claim in the treatment of disease.

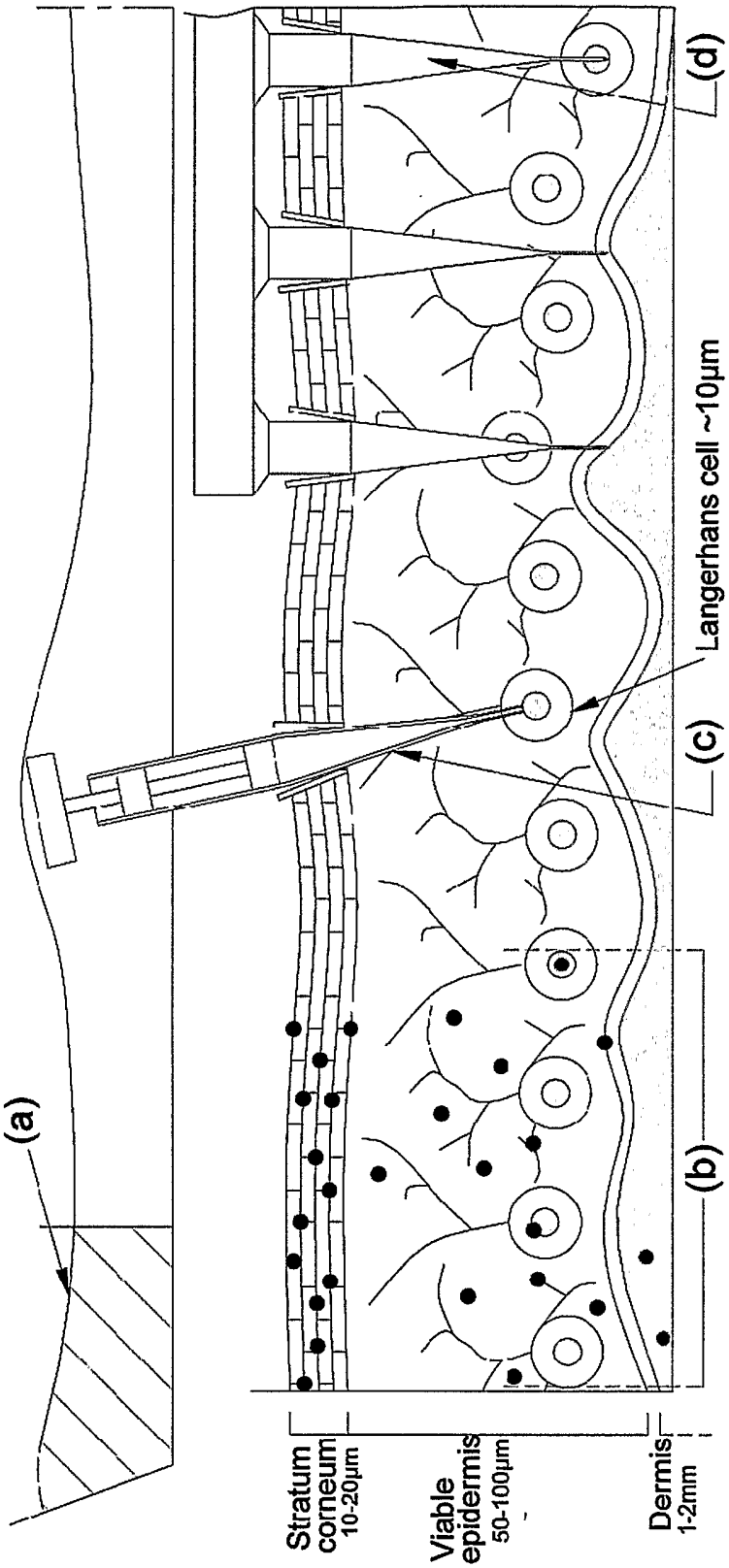
(a)
(b)
(c)
(d)
Langerhans cell ~10µm
Stratum corneum 10-20µm
Viable epidermis 50-100µm
Dermis 1-2mm

FIG. 1

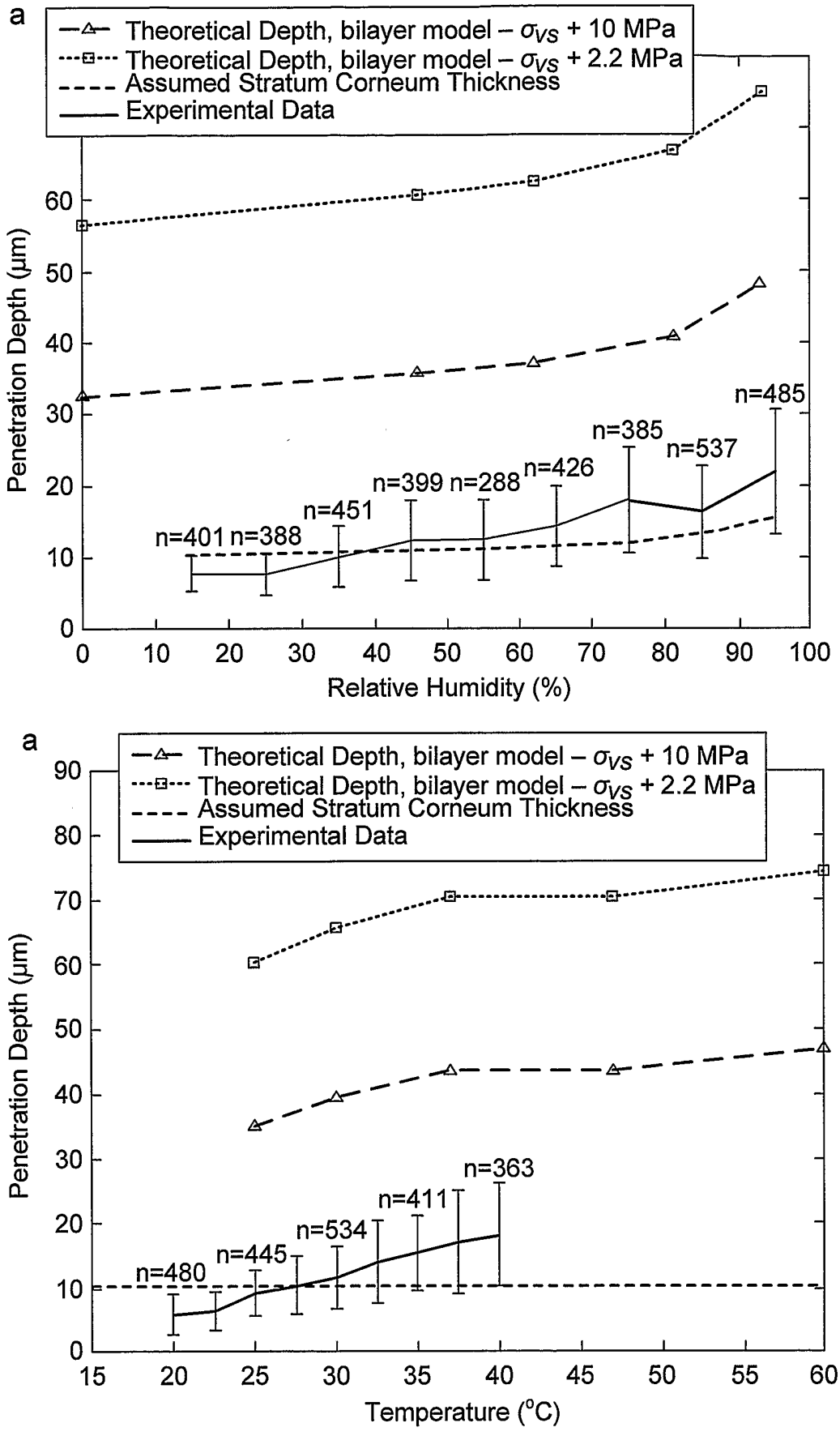
a
Theoretical Depth, bilayer model – σ_{VS} + 10 MPa
Theoretical Depth, bilayer model – σ_{VS} + 2.2 MPa
Assumed Stratum Corneum Thickness
Experimental Data
Penetration Depth (μm)
Relative Humidity (%)
n=401 n=388
n=451
n=399 n=288
n=426
n=385
n=537
n=485
a
Theoretical Depth, bilayer model – σ_{VS} + 10 MPa
Theoretical Depth, bilayer model – σ_{VS} + 2.2 MPa
Assumed Stratum Corneum Thickness
Experimental Data
Penetration Depth (μm)
Temperature (°C)
n=480
n=445
n=534
n=411
n=363

FIG. 2

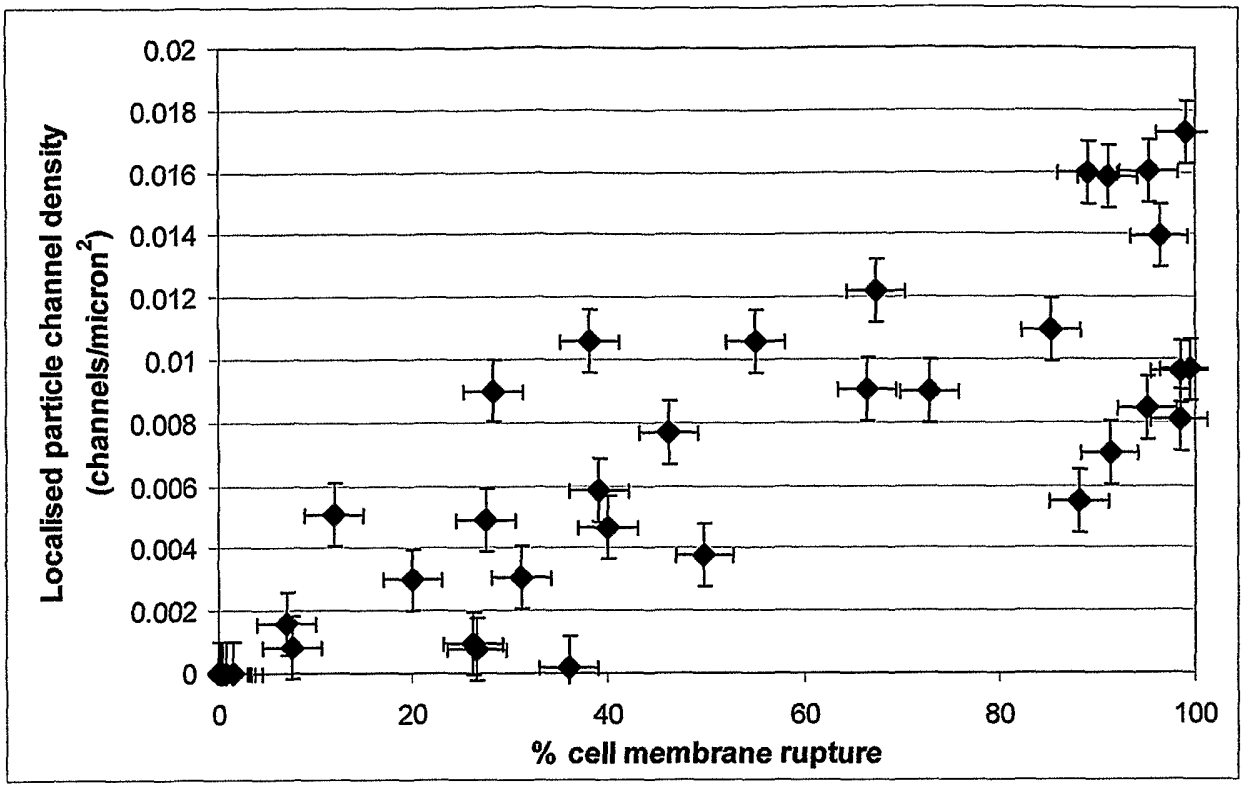
Localised particle channel density (channels/micron²)
0.02
0.018
0.016
0.014
0.012
0.01
0.008
0.006
0.004
0.002
0
0
20
40
60
80
100
% cell membrane rupture

(a)

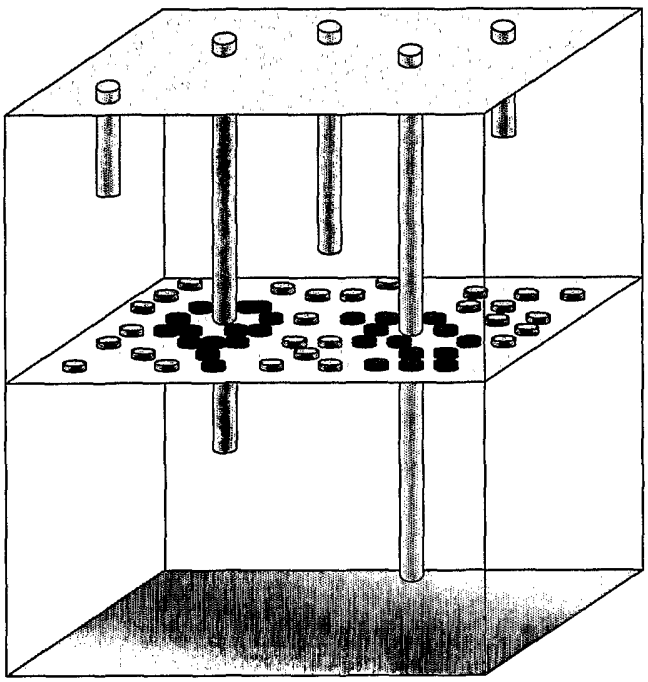

(b)

FIG. 3

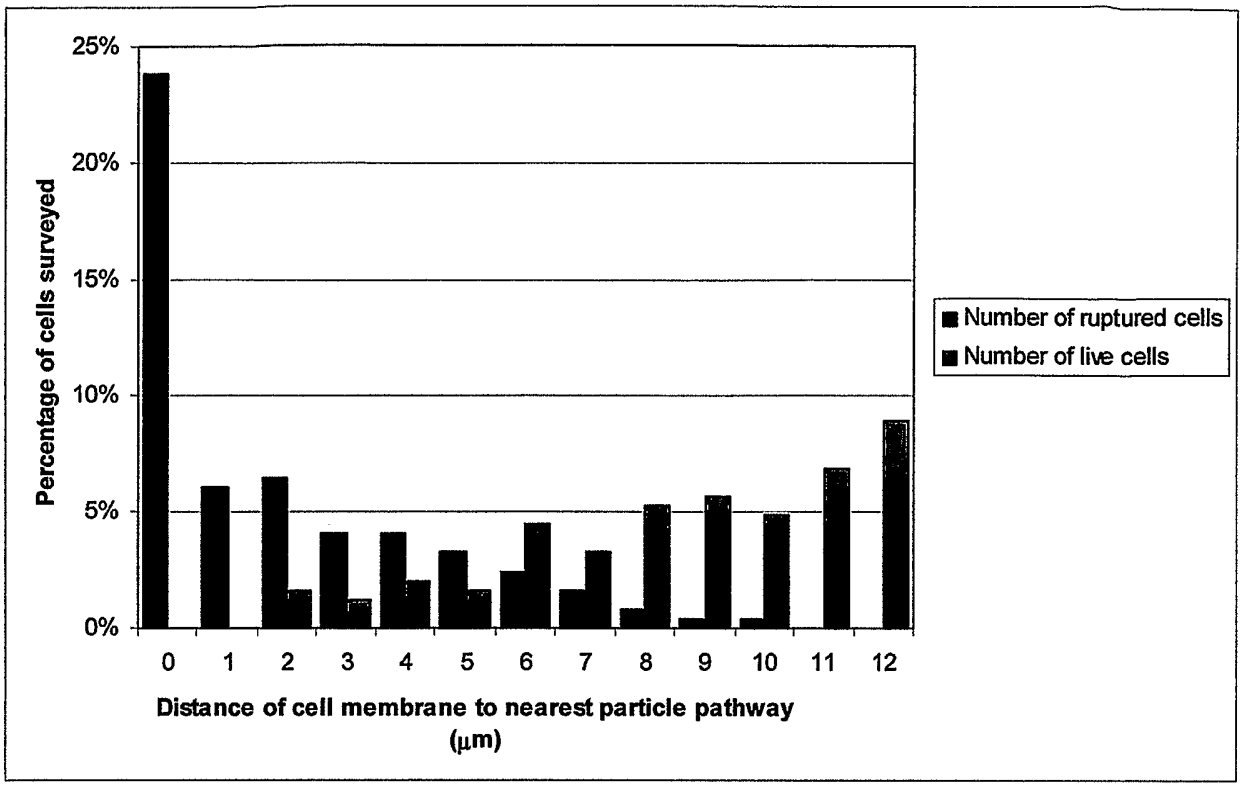
25%
20%
15%
10%
5%
0%
Percentage of cells surveyed
0 1 2 3 4 5 6 7 8 9 10 11 12
Distance of cell membrane to nearest particle pathway (μm)
Number of ruptured cells
Number of live cells

(c)

FIG. 3

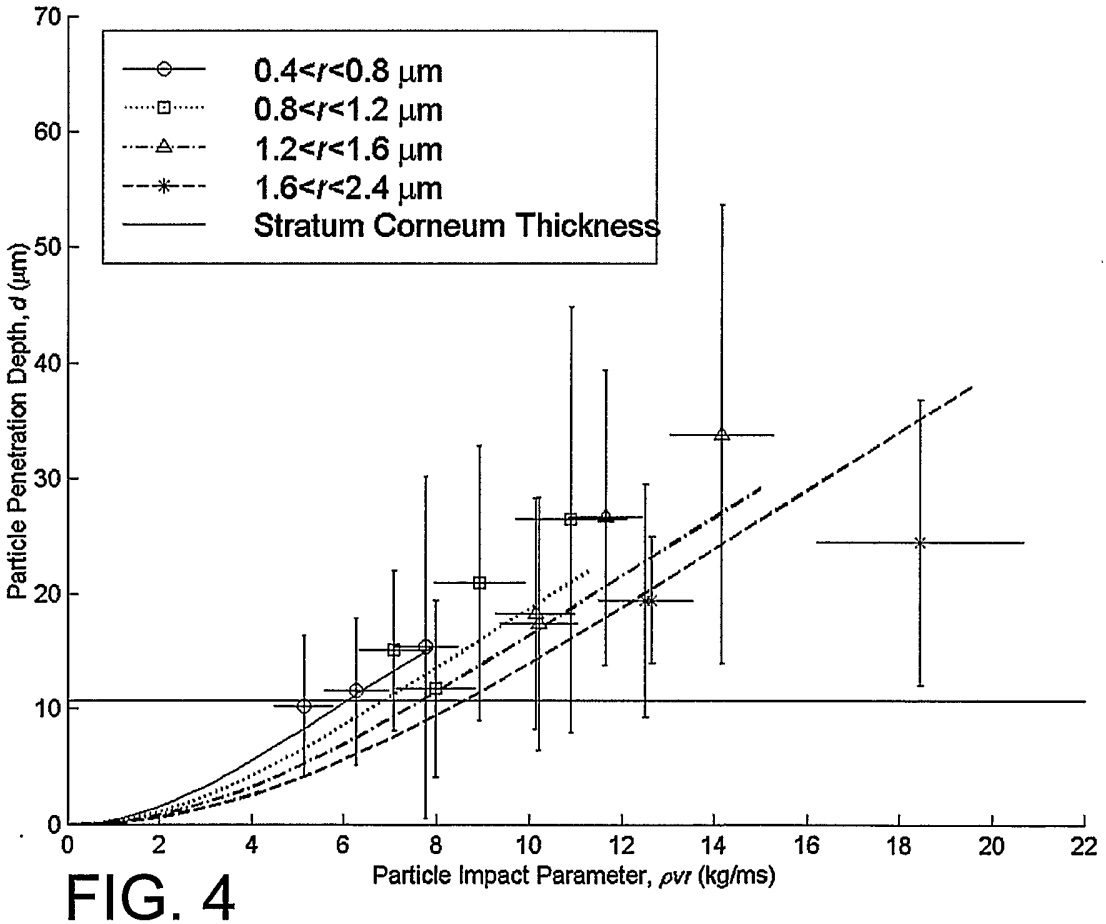
0.4<r<0.8 μm
0.8<r<1.2 μm
1.2<r<1.6 μm
1.6<r<2.4 μm
Stratum Corneum Thickness
Particle Penetration Depth, d (μm)
Particle Impact Parameter, ρvr (kg/ms)
0 2 4 6 8 10 12 14 16 18 20 22
0 10 20 30 40 50 60 70

FIG. 4

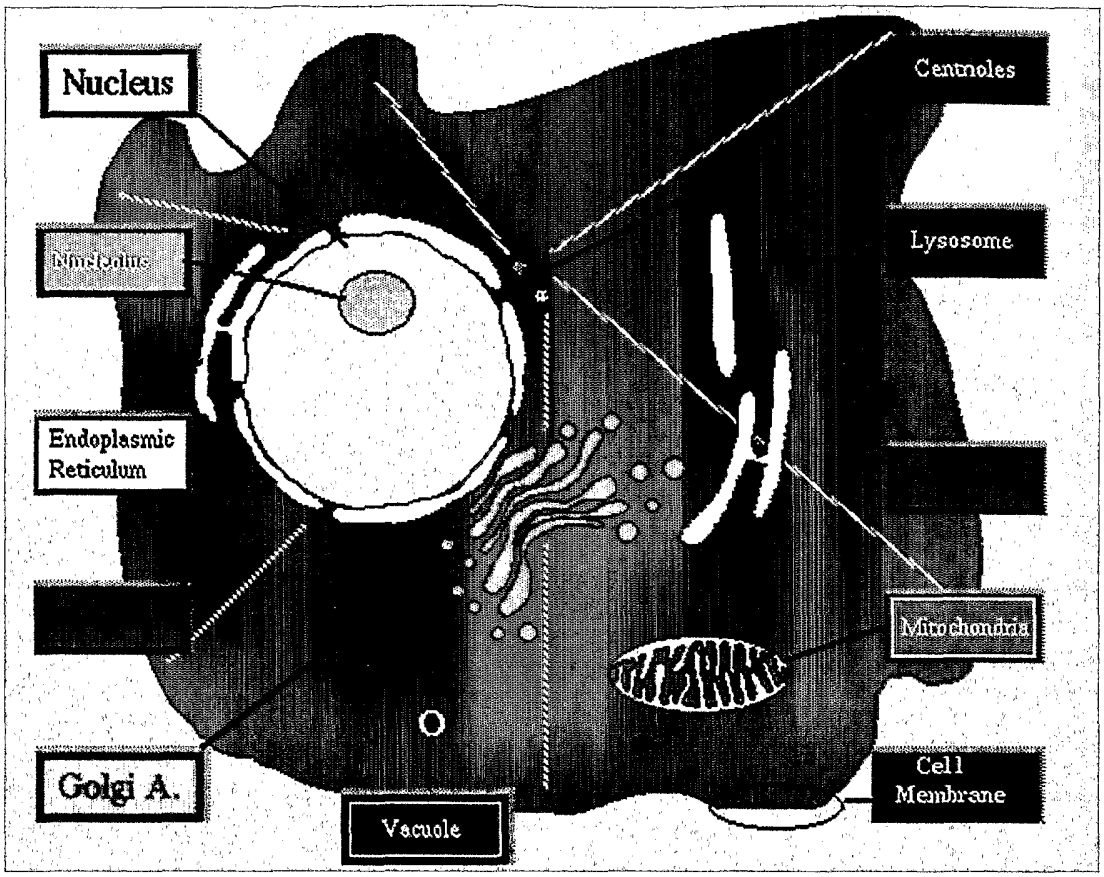
Nucleus
Centrioles
Lysosome
Endoplasmic Reticulum
Mitochondria
Golgi A.
Vacuole
Cell Membrane

FIG. 5

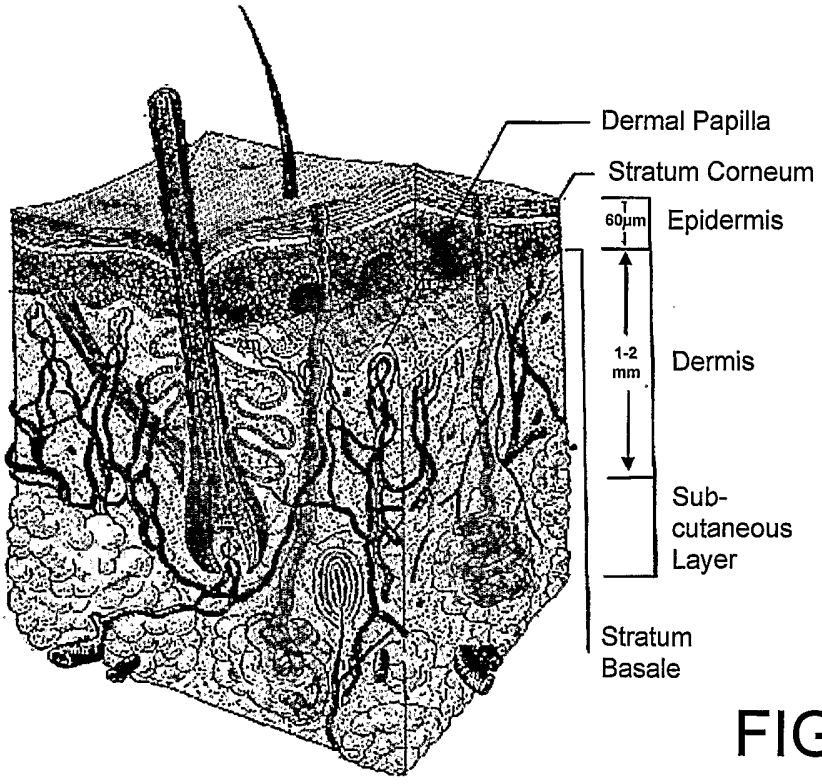
Dermal Papilla
Stratum Corneum
60µm
Epidermis
1-2 mm
Dermis
Sub-cutaneous Layer
Stratum Basale

FIG. 6

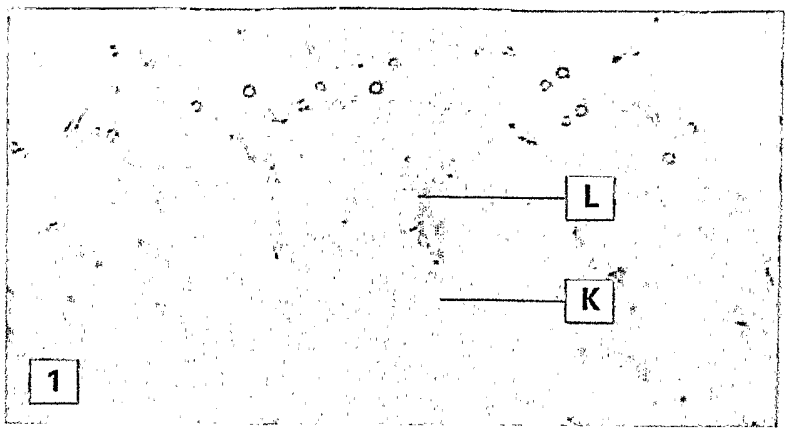

FIG. 7

FIG. 8

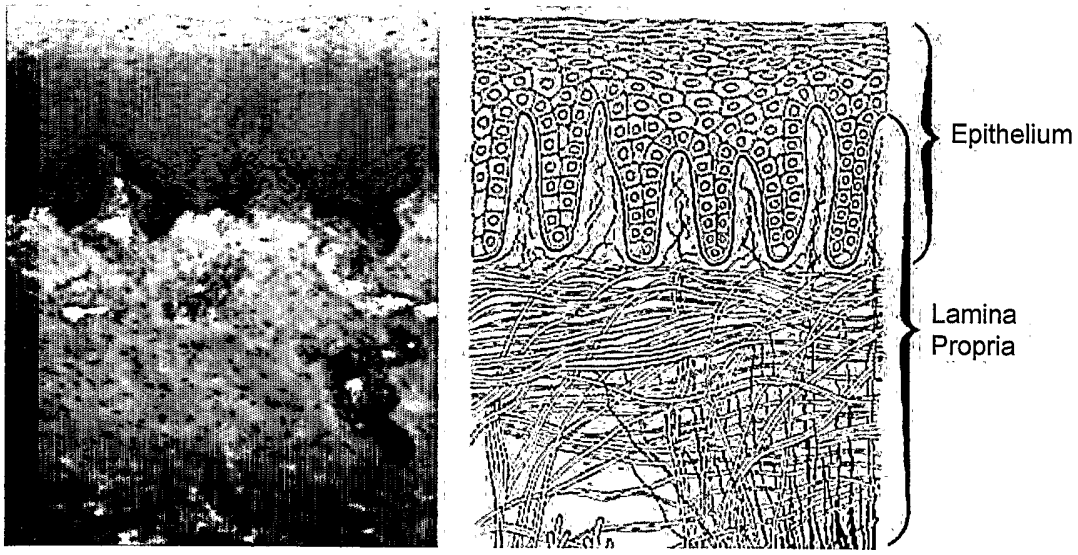

FIG. 9

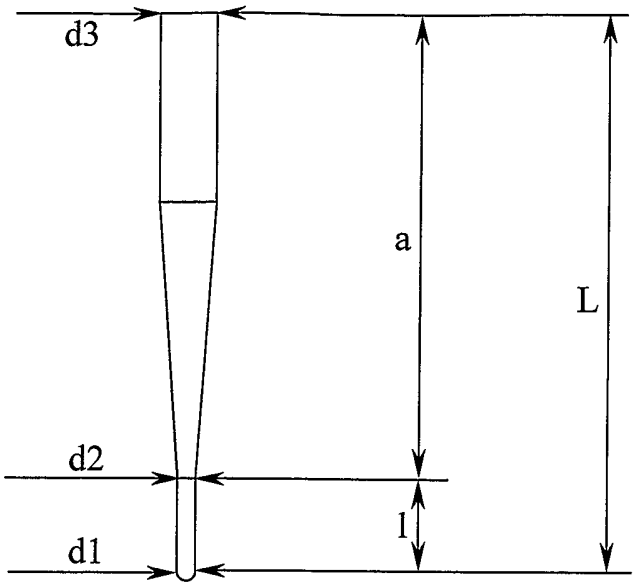
d3
a
L
d2
l
d1

FIG. 10

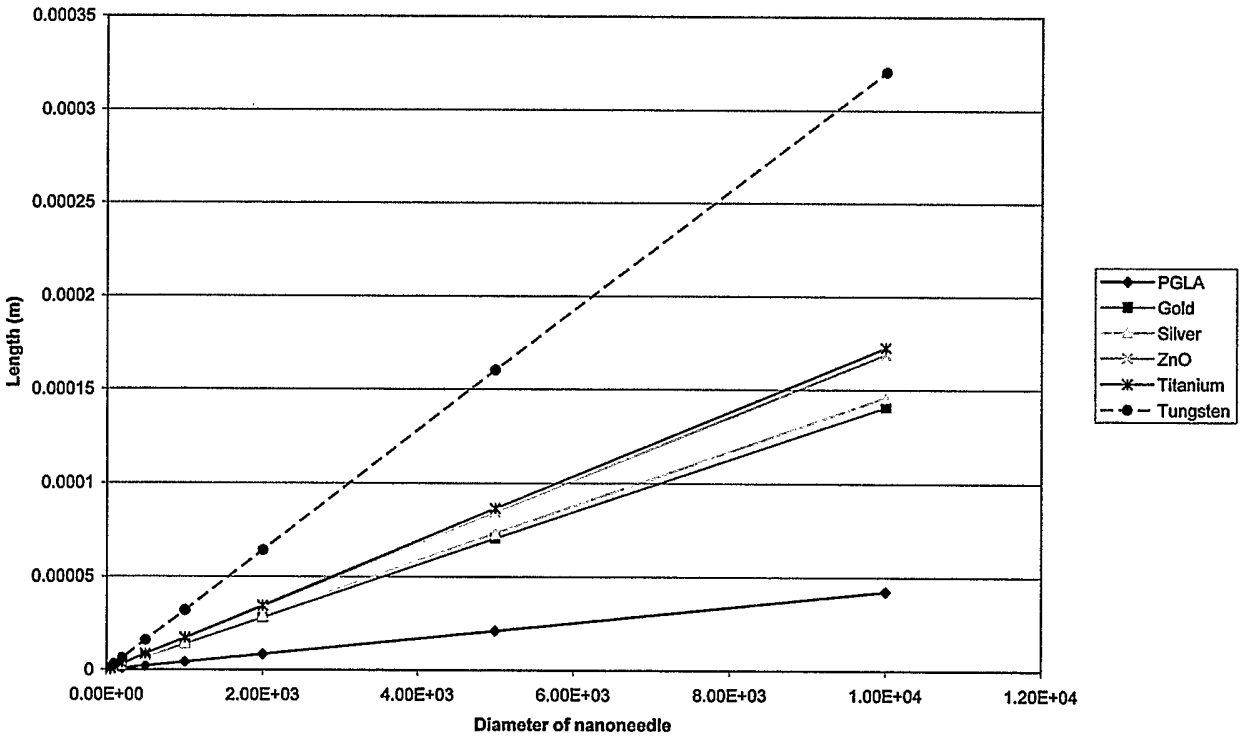
0.00035
0.0003
0.00025
0.0002
0.00015
0.0001
0.00005
0
Length (m)
0.00E+00
2.00E+03
4.00E+03
6.00E+03
8.00E+03
1.00E+04
1.20E+04
Diameter of nanoneedle
PGLA
Gold
Silver
ZnO
Titanium
Tungsten

FIG. 11

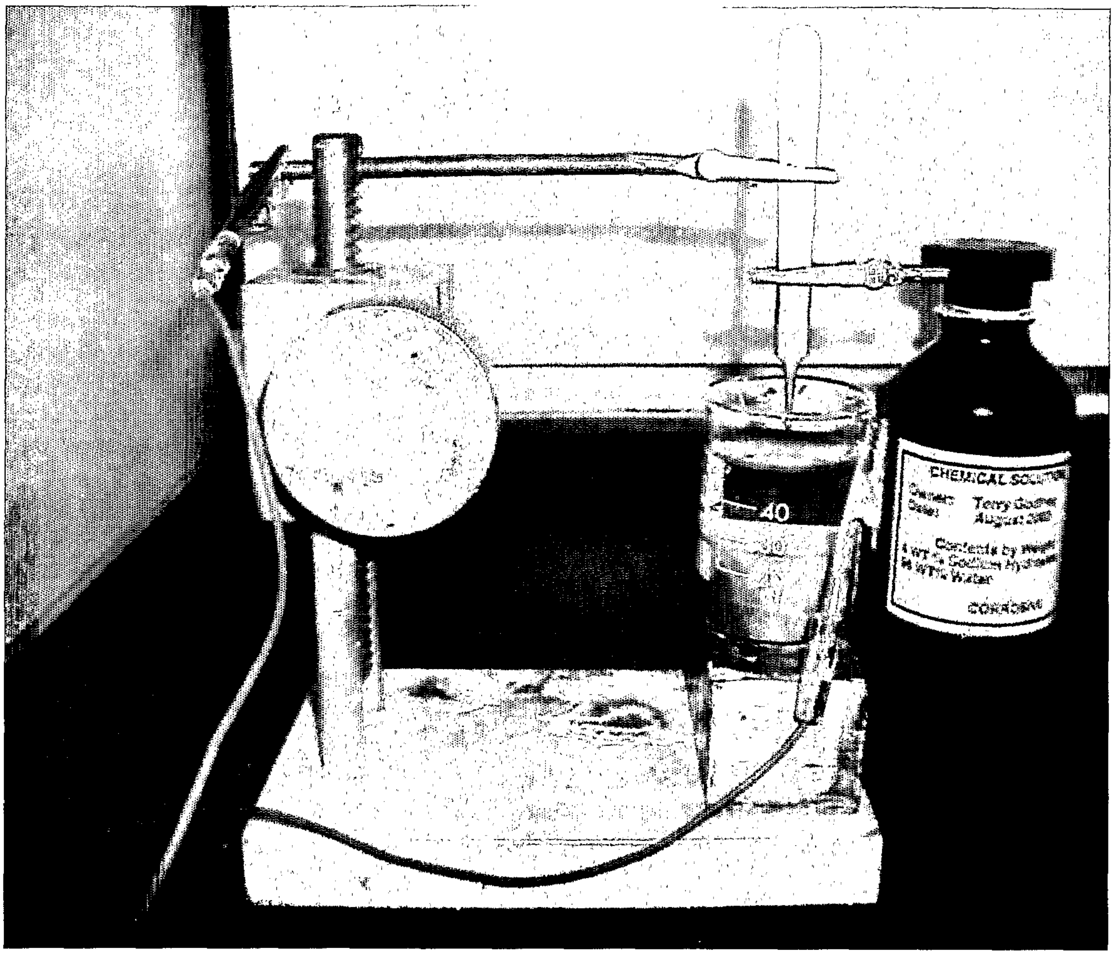

FIG. 12

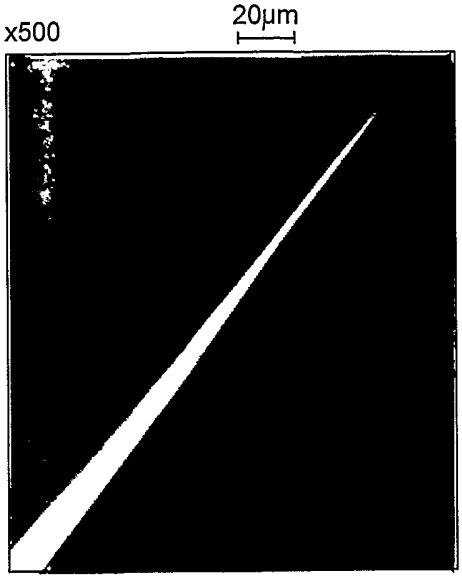

(a)

(b)

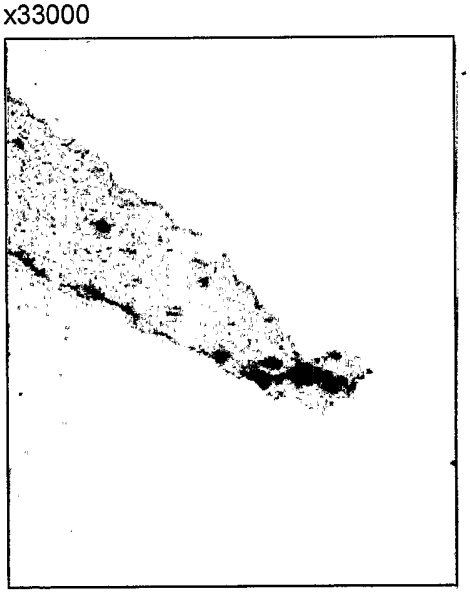

(c)

FIG. 13

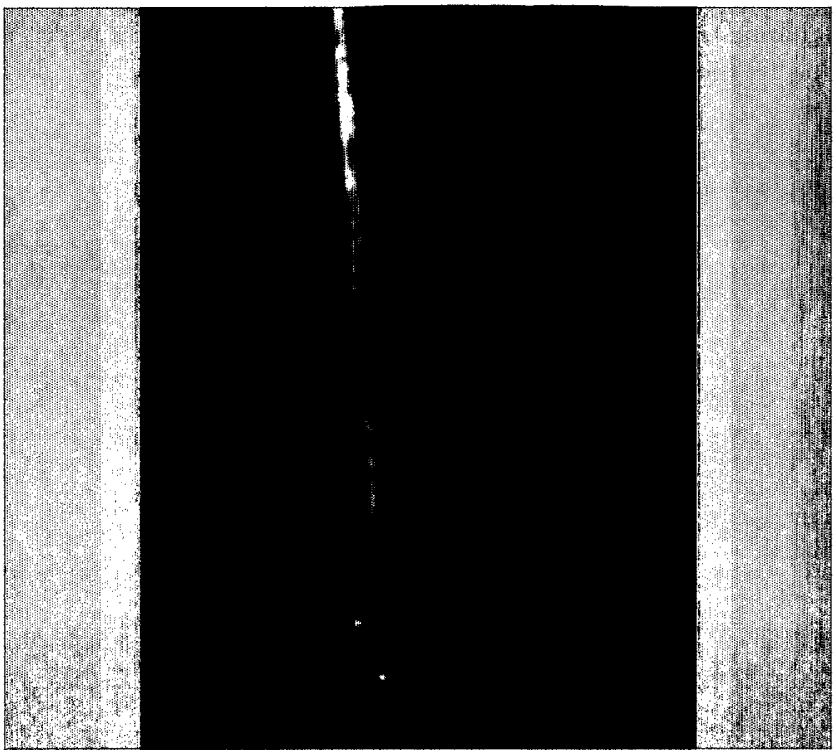

(a)

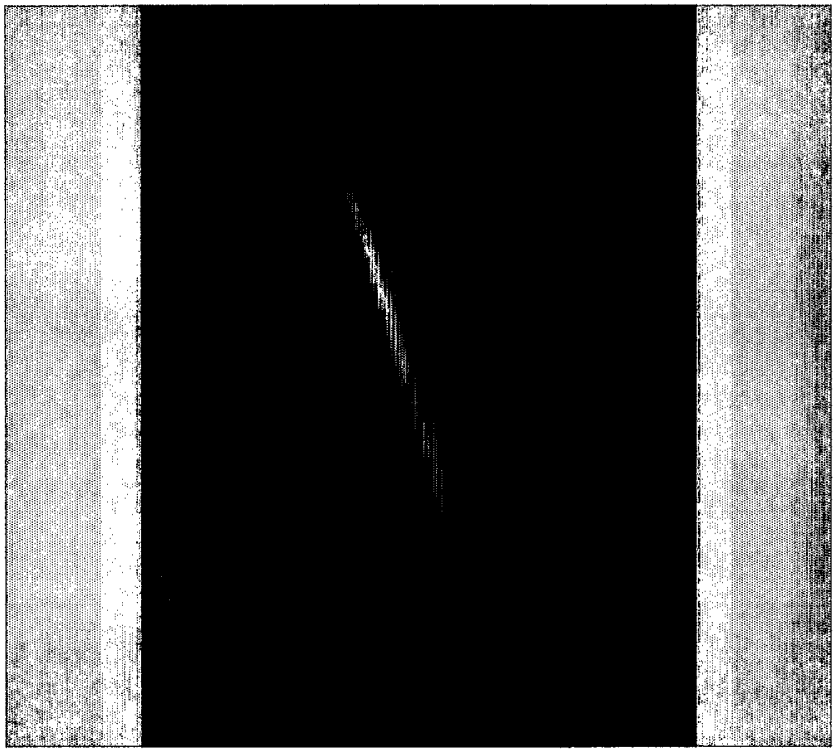

(b)

FIG. 14

(a)

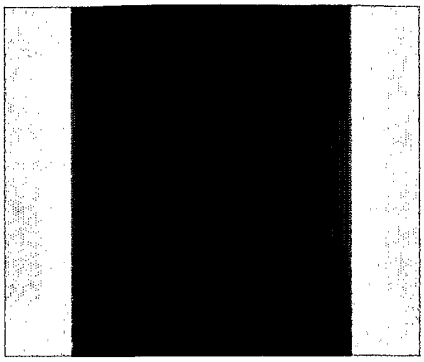

(b)

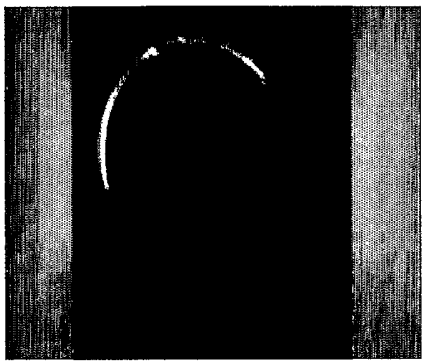

(c)

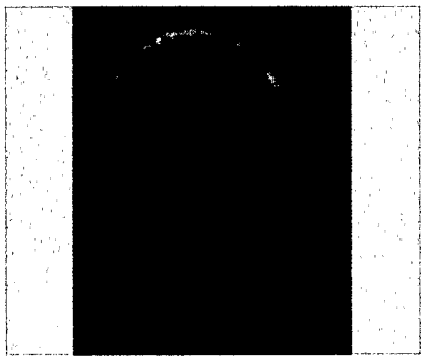

(d)

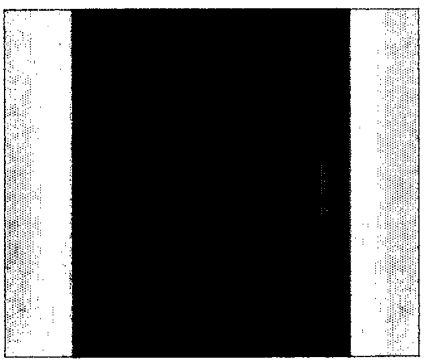

FIG. 15

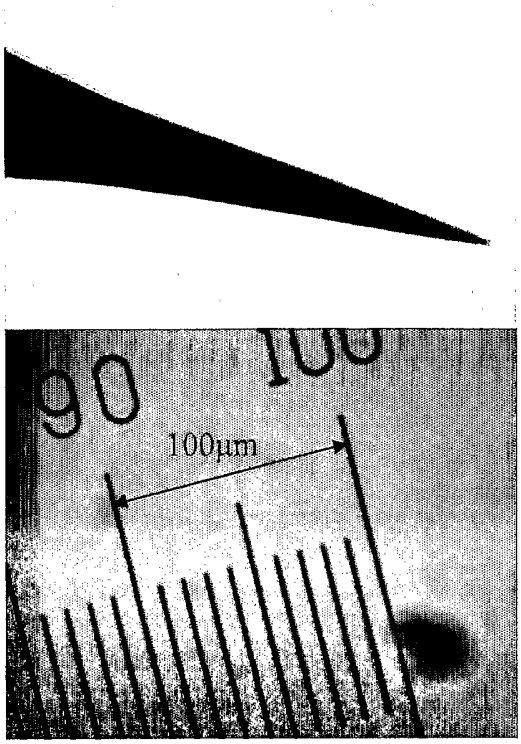
90
100µm

FIG. 16

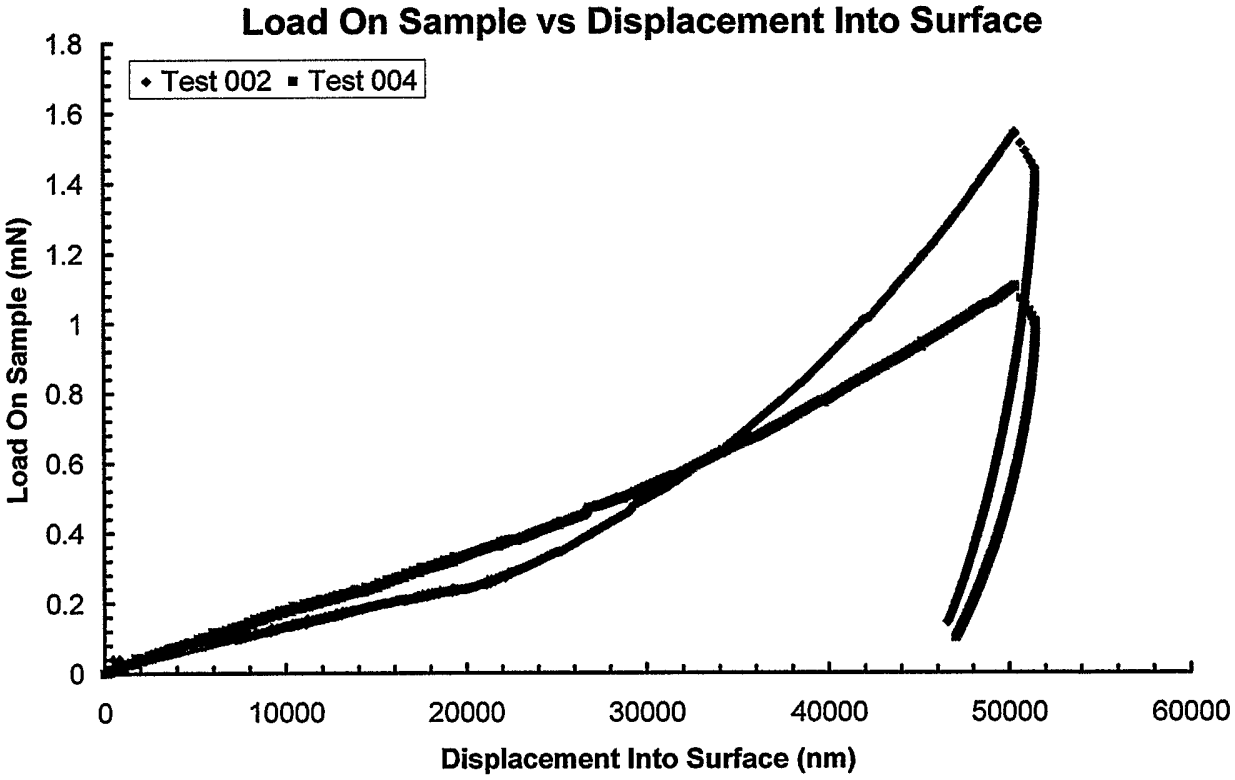
Load On Sample vs Displacement Into Surface
Test 002
Test 004
Load On Sample (mN)
1.8
1.6
1.4
1.2
1
0.8
0.6
0.4
0.2
0
0
10000
20000
30000
40000
50000
60000
Displacement Into Surface (nm)

FIG. 17

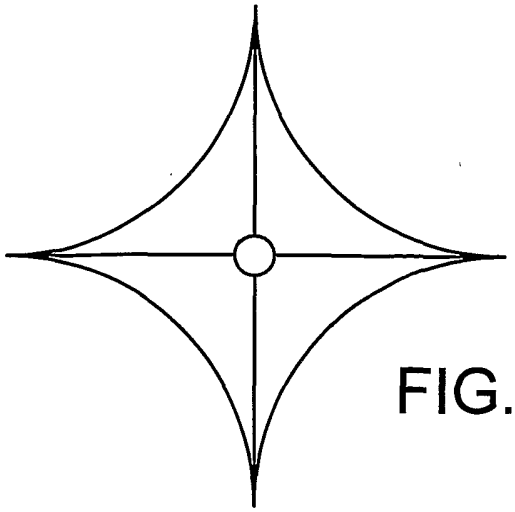

FIG. 18

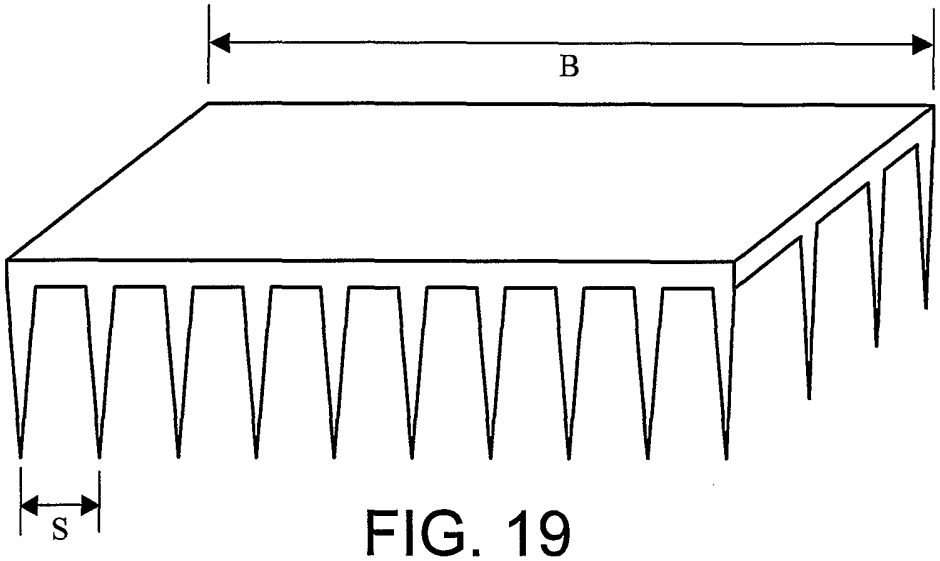

FIG. 19

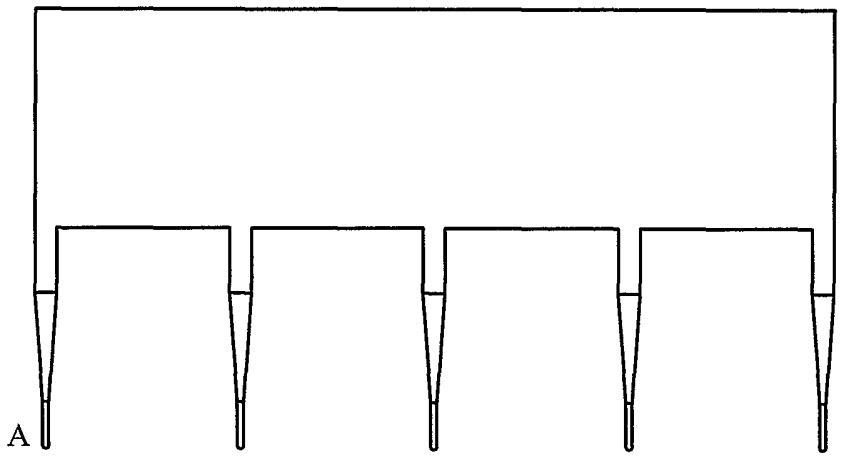

FIG. 20

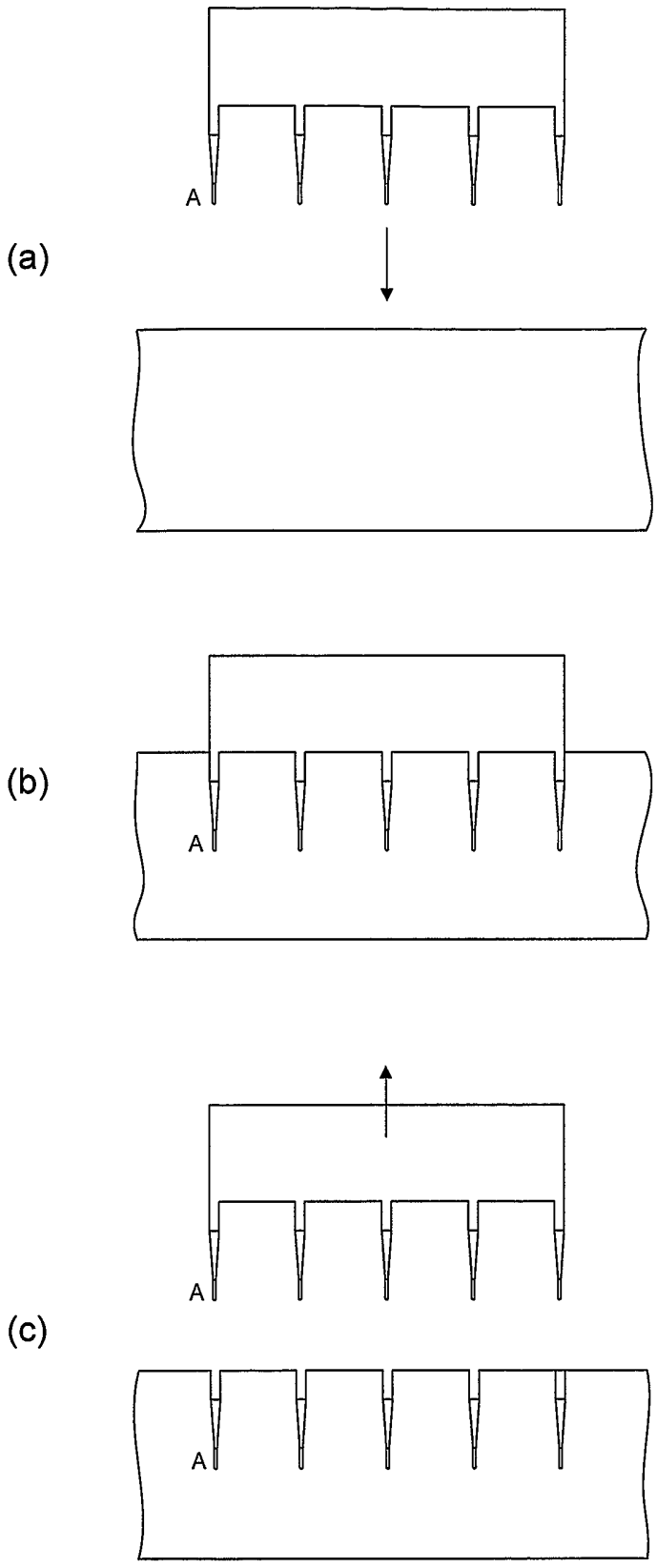

FIG. 21

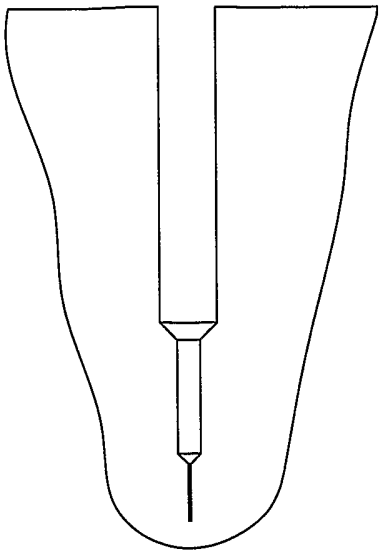

FIG. 22

(a)

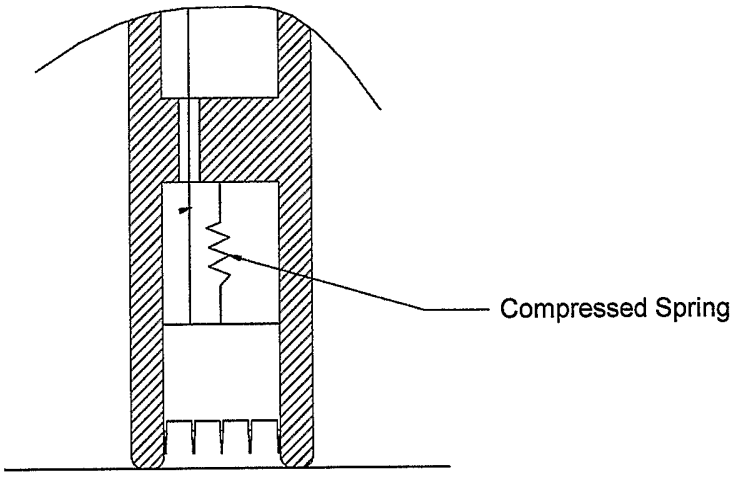

FIG. 23

(b)

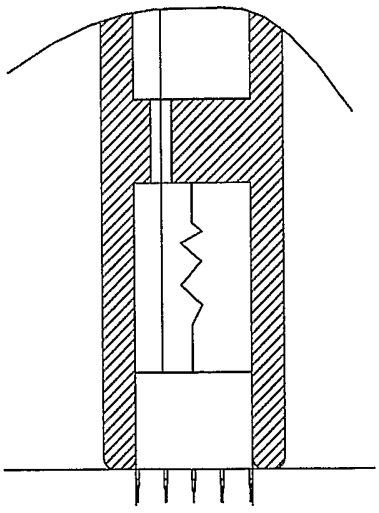

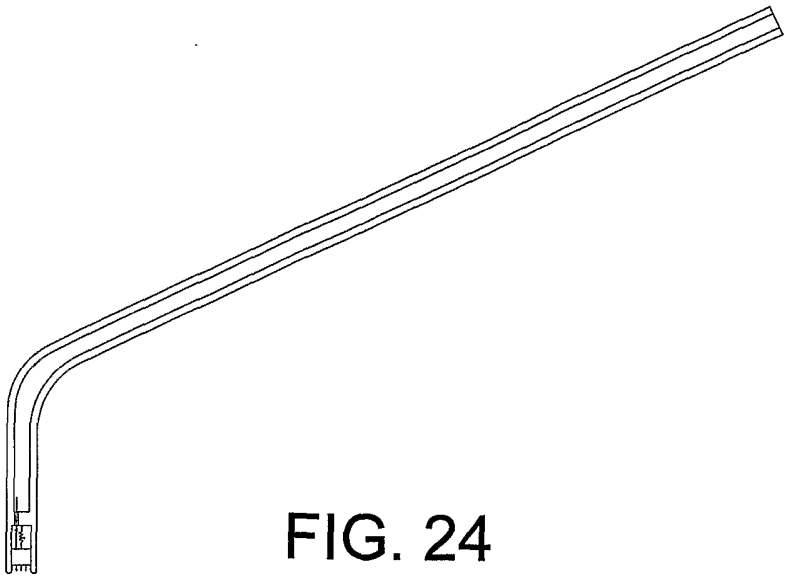

FIG. 24

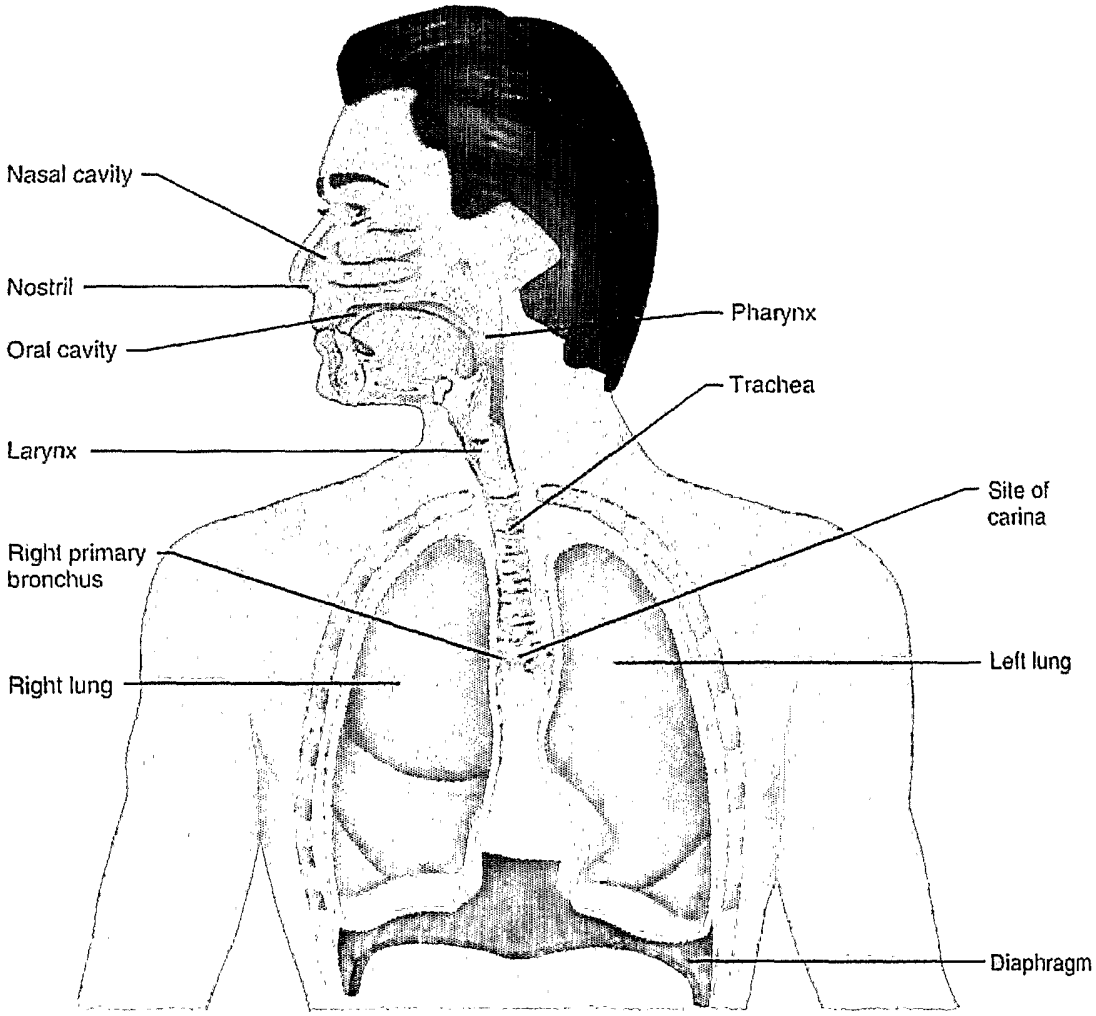
Nasal cavity
Nostril
Oral cavity
Larynx
Right primary bronchus
Right lung
Pharynx
Trachea
Site of carina
Left lung
Diaphragm

FIG. 25

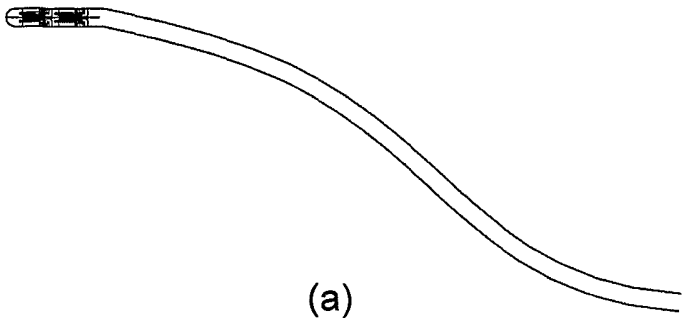

(a)

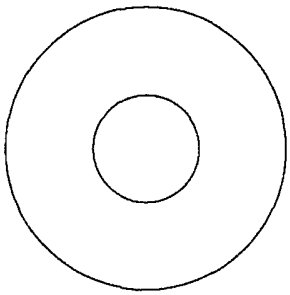

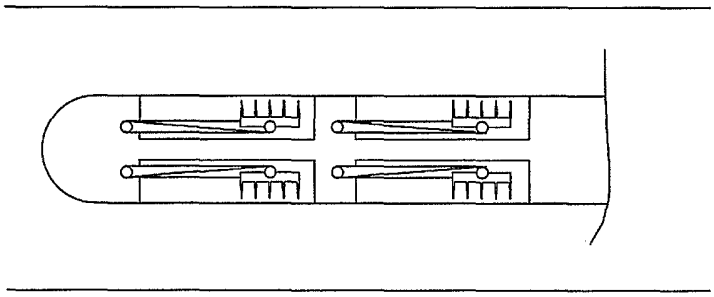

(b)

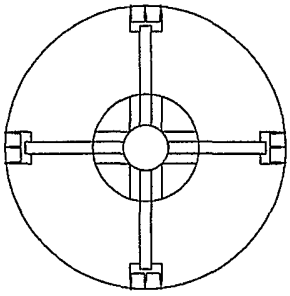

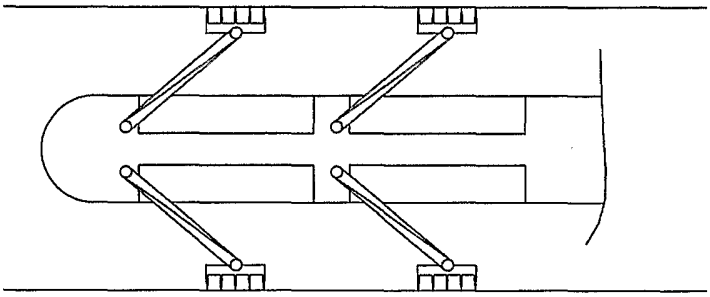

(c)

FIG. 26

INTERNATIONAL SEARCH REPORT

International Application No
PCT/GB2005/000336

A. CLASSIFICATION OF SUBJECT MATTER
IPC 7 A61B17/20 A61M37/00

According to International Patent Classification (IPC) or to both national classification and IPC

B. FIELDS SEARCHED

Minimum documentation searched (classification system followed by classification symbols)
IPC 7 A61B A61M

Documentation searched other than minimum documentation to the extent that such documents are included in the fields searched

Electronic data base consulted during the international search (name of data base and, where practical, search terms used)
EPO-Internal

C. DOCUMENTS CONSIDERED TO BE RELEVANT

Category °	Citation of document, with indication, where appropriate, of the relevant passages	Relevant to claim No.
X	US 5 457 041 A (GINAVEN ET AL) 10 October 1995 (1995-10-10) column 7, line 1 - column 8, line 23; figures 1,4b	1-44
X	WO 02/064193 A (GEORGIA TECH RESEARCH CORPORATION) 22 August 2002 (2002-08-22) page 9, line 1 page 10, line 3 - page 11, line 13; figures 10,12	1-44
X	WO 2004/000389 A (KWON, SUNG-YUN) 31 December 2003 (2003-12-31) page 5, line 5 - page 6, line 21; figures 1-3	1-44

-/--

[X] Further documents are listed in the continuation of box C.

[X] Patent family members are listed in annex.

° Special categories of cited documents :

"A" document defining the general state of the art which is not considered to be of particular relevance

"E" earlier document but published on or after the international filing date

"L" document which may throw doubts on priority claim(s) or which is cited to establish the publication date of another citation or other special reason (as specified)

"O" document referring to an oral disclosure, use, exhibition or other means

"P" document published prior to the international filing date but later than the priority date claimed

"T" later document published after the international filing date or priority date and not in conflict with the application but cited to understand the principle or theory underlying the invention

"X" document of particular relevance; the claimed invention cannot be considered novel or cannot be considered to involve an inventive step when the document is taken alone

"Y" document of particular relevance; the claimed invention cannot be considered to involve an inventive step when the document is combined with one or more other such documents, such combination being obvious to a person skilled in the art.

"&" document member of the same patent family

Date of the actual completion of the international search	Date of mailing of the international search report
12 May 2005	24/05/2005

Name and mailing address of the ISA	Authorized officer
European Patent Office, P.B. 5818 Patentlaan 2 NL – 2280 HV Rijswijk Tel. (+31–70) 340–2040, Tx. 31 651 epo nl, Fax: (+31–70) 340–3016	Moers, R

1

Form PCT/ISA/210 (second sheet) (January 2004)

INTERNATIONAL SEARCH REPORT

International Application No
PCT/GB2005/000336

C.(Continuation) DOCUMENTS CONSIDERED TO BE RELEVANT

Category °	Citation of document, with indication, where appropriate, of the relevant passages	Relevant to claim No.
X	US 6 503 231 B1 (PRAUSNITZ MARK R ET AL) 7 January 2003 (2003-01-07) cited in the application column 5, line 19 column 5, line 39 - column 6, line 18 column 9, line 66 - column 10, line 6; figures 2-4	1-44
X	WO 02/100476 A (BECTON, DICKINSON AND COMPANY; MARTIN, FRANK, E; EVANS, JOHN, D) 19 December 2002 (2002-12-19) cited in the application page 5, line 1 - line 18; figure 1	1

1

INTERNATIONAL SEARCH REPORT

ıational application No.
PCT/GB2005/000336

Box II Observations where certain claims were found unsearchable (Continuation of item 2 of first sheet)

This International Search Report has not been established in respect of certain claims under Article 17(2)(a) for the following reasons:

1. [X] Claims Nos.: 45
because they relate to subject matter not required to be searched by this Authority, namely:

Rule 39.1(iv) PCT - Method for treatment of the human or animal body by surgery

2. [ ] Claims Nos.:
because they relate to parts of the International Application that do not comply with the prescribed requirements to such an extent that no meaningful International Search can be carried out, specifically:

3. [ ] Claims Nos.:
because they are dependent claims and are not drafted in accordance with the second and third sentences of Rule 6.4(a).

Box III Observations where unity of invention is lacking (Continuation of item 3 of first sheet)

This International Searching Authority found multiple inventions in this international application, as follows:

1. [ ] As all required additional search fees were timely paid by the applicant, this International Search Report covers all searchable claims.

2. [ ] As all searchable claims could be searched without effort justifying an additional fee, this Authority did not invite payment of any additional fee.

3. [ ] As only some of the required additional search fees were timely paid by the applicant, this International Search Report covers only those claims for which fees were paid, specifically claims Nos.:

4. [ ] No required additional search fees were timely paid by the applicant. Consequently, this International Search Report is restricted to the invention first mentioned in the claims; it is covered by claims Nos.:

Remark on Protest

[ ] The additional search fees were accompanied by the applicant's protest.

[ ] No protest accompanied the payment of additional search fees.

INTERNATIONAL SEARCH REPORT

Information on patent family members

International Application No
PCT/GB2005/000336

Patent document cited in search report		Publication date	Patent family member(s)		Publication date
US 5457041	A	10-10-1995	NONE		
WO 02064193	A	22-08-2002	EP	1345646 A2	24-09-2003
			WO	02064193 A2	22-08-2002
			US	2002082543 A1	27-06-2002
WO 2004000389	A	31-12-2003	US	2004087893 A1	06-05-2004
			AU	2003243750 A1	06-01-2004
			CA	2490137 A1	31-12-2003
			WO	2004000389 A2	31-12-2003
			US	2004199103 A1	07-10-2004
			AU	2003275311 A1	30-04-2004
			WO	2004024224 A1	25-03-2004
US 6503231	B1	07-01-2003	AU	767122 B2	30-10-2003
			AU	4561699 A	30-12-1999
			AU	2004200303 A1	19-02-2004
			CA	2330207 A1	16-12-1999
			EP	1086214 A1	28-03-2001
			JP	2002517300 T	18-06-2002
			US	2002138049 A1	26-09-2002
			WO	9964580 A1	16-12-1999
			US	6334856 B1	01-01-2002
WO 02100476	A	19-12-2002	EP	1395328 A2	10-03-2004
			JP	2004532698 T	28-10-2004
			WO	02100476 A2	19-12-2002
			US	2002188245 A1	12-12-2002